

https://dspace.org/

Performance of filter drains under large embankment loads

Rumpelt, Thomas Karl

2015-09-09
http://hdl.handle.net/10539/18591

Downloaded from a DSpace repository. https://dspace.org/

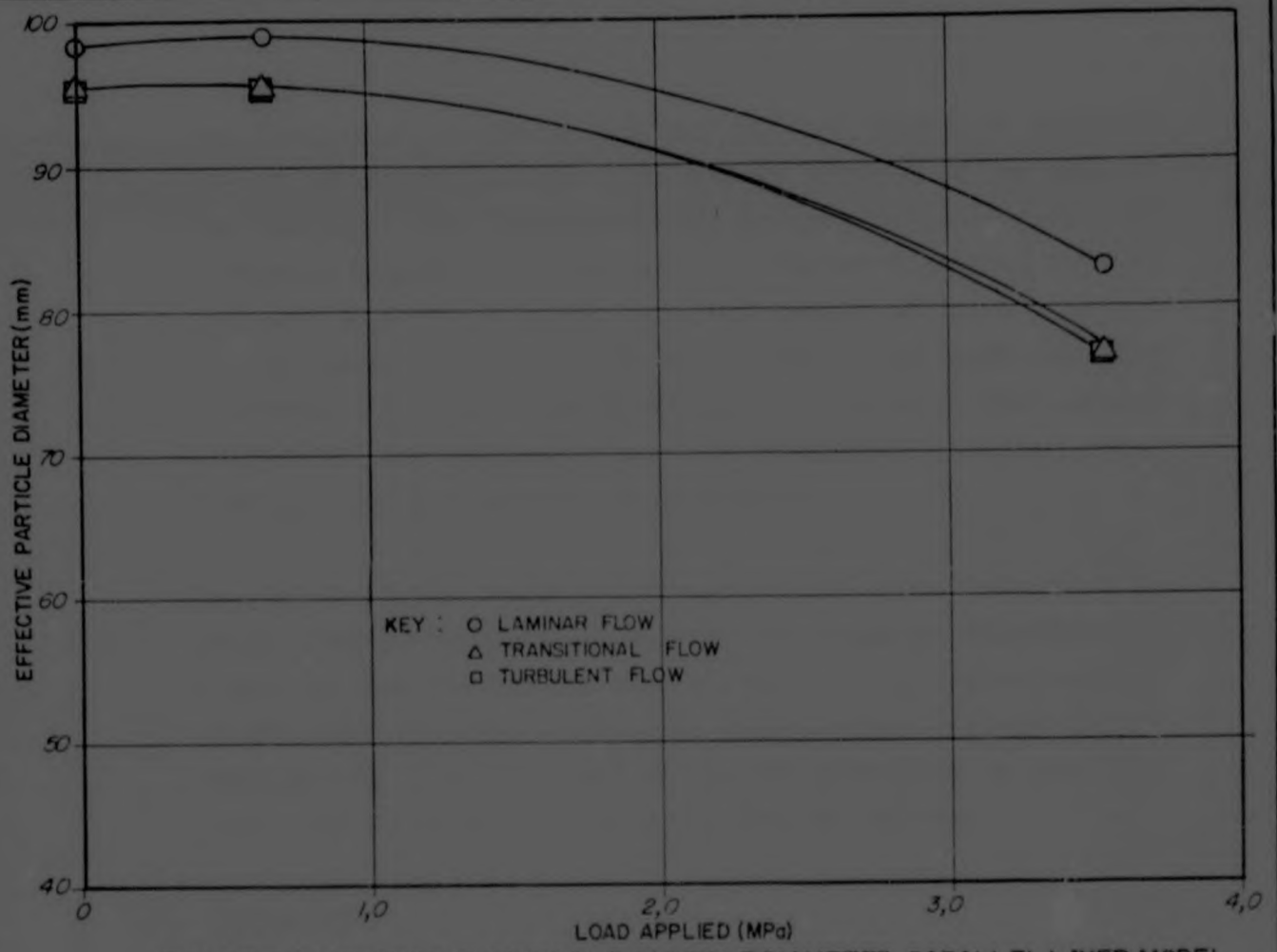


FIGURE 6.2a CHANGE IN EFFECTIVE PARTICLE DIAMETER-PARALLEL LAYER MODEL

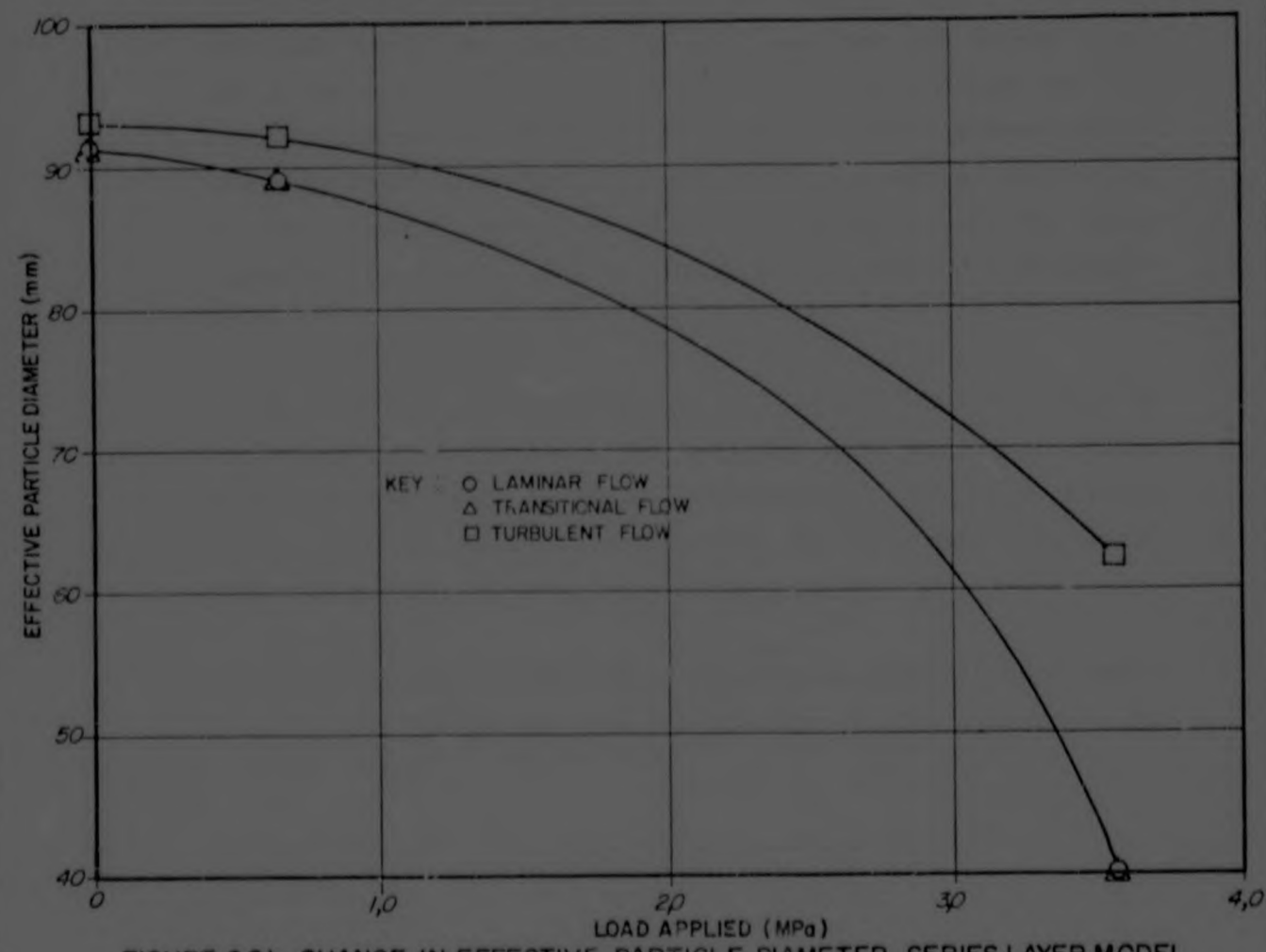


FIGURE 6.2b CHANGE IN EFFECTIVE PARTICLE DIAMETER-SERIES LAYER MODEL

The load tests therefore had the combined effect of reducing the effective particle diameter and the porosity of the sample. The change in flow characteristics is therefore as a result of a change in both these parameters. Further changes, such as the average particle shape, were not considered here, although it was observed that a large portion of broken particles were elongated. It will be difficult to quantify this change rationally, as particle shape and roughness are dealt with qualitatively and empirically at present.

The effect of the change in porosity or effective particle diameter alone on the flow characteristics could be determined in remoulded samples with the same porosity as the initial sample. If the shape and hence packing of the particles does not change considerably after the load tests, the remoulding to the initial porosity should be relatively easy to achieve.

6.4 Porosities

In calculating the porosities of the sample during and after the load tests, the assumption was made that the stress level and hence amount of settlement and particle breakage was the same throughout the depth of the sample. For a uniform stress level to exist throughout the depth of the sample, the lining of the cylinder must not allow the transfer of any shear stresses to the wall, ie the lining must be perfectly frictionless.

Movement in the lower portion of the cylinder was evidenced by the signs of distress in the cylinder wall at higher loads. Although this does not form conclusive evidence of a uniform stress level throughout the cylinder, it vindicates the use of that assumption, if only for want of a better alternative.

The specimen was handpacked, resulting in a fairly high porosity of 0,49 before any load was applied to the specimen. The

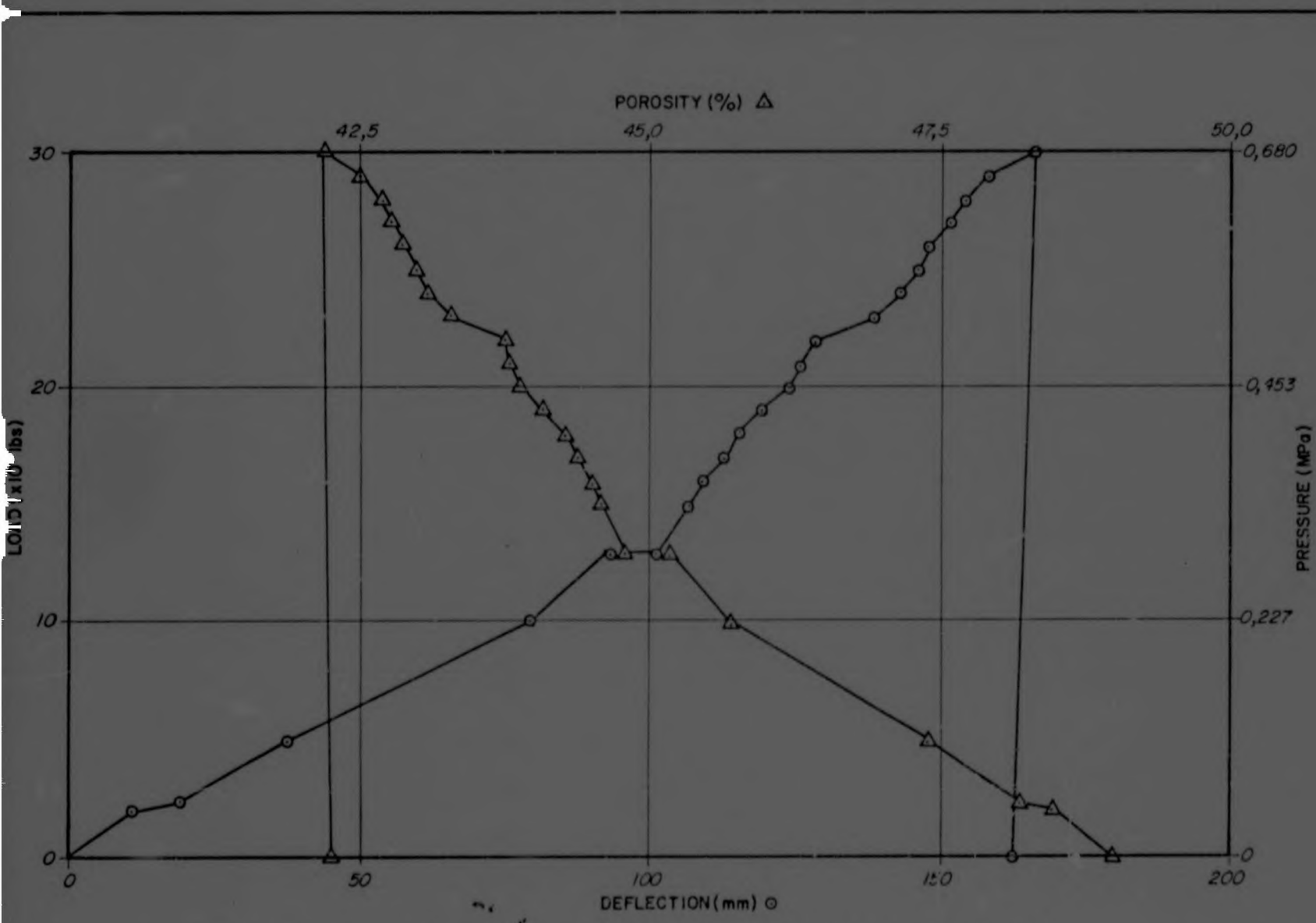


FIGURE 6.3 PLOT OF LOAD & PRESSURE vs DEFLECTION & POROSITY FOR LOAD TEST No I

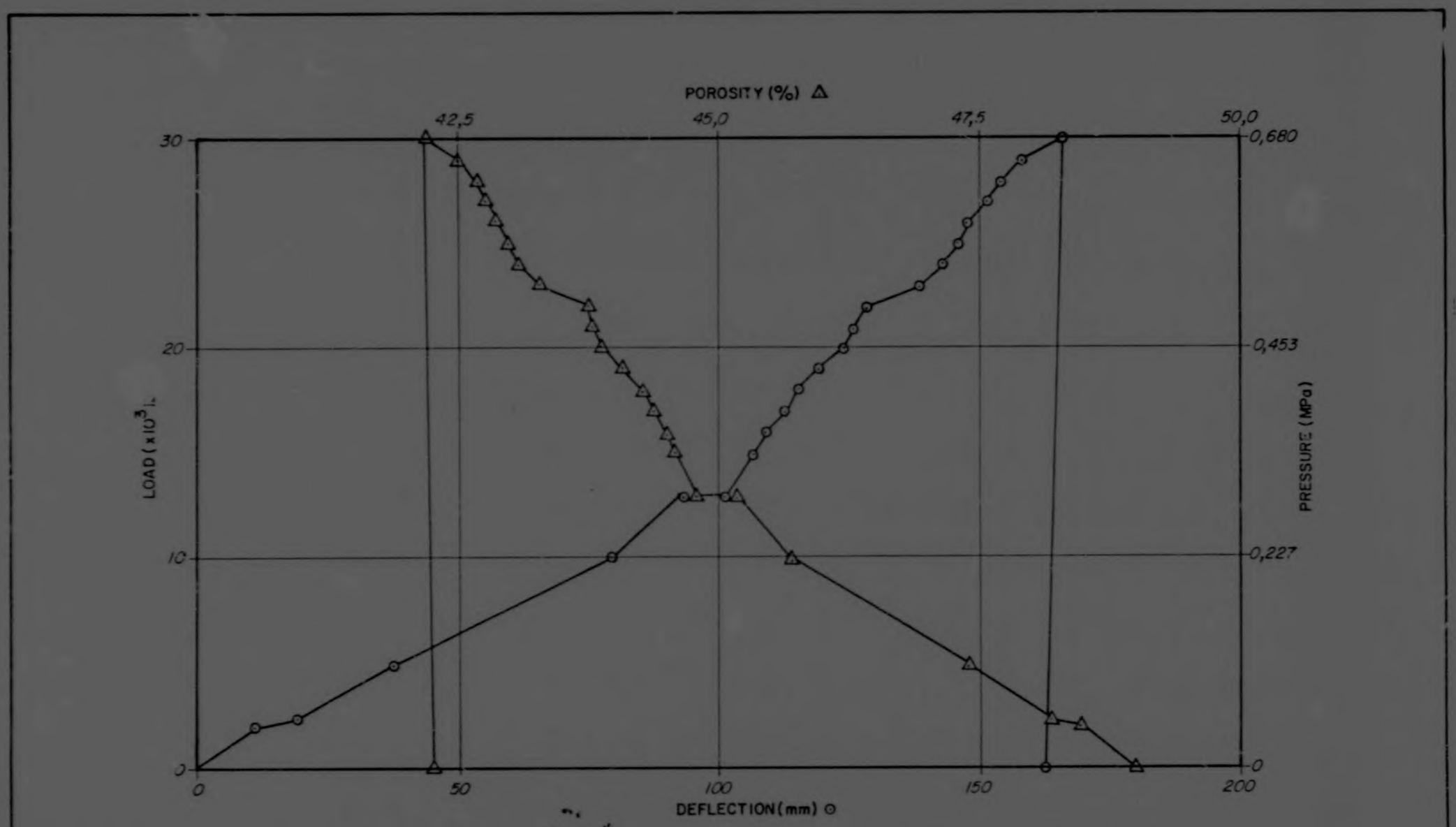


FIGURE 6.3 PLOT OF LOAD & PRESSURE vs DEFLECTION & POROSITY FOR LOAD TEST No I

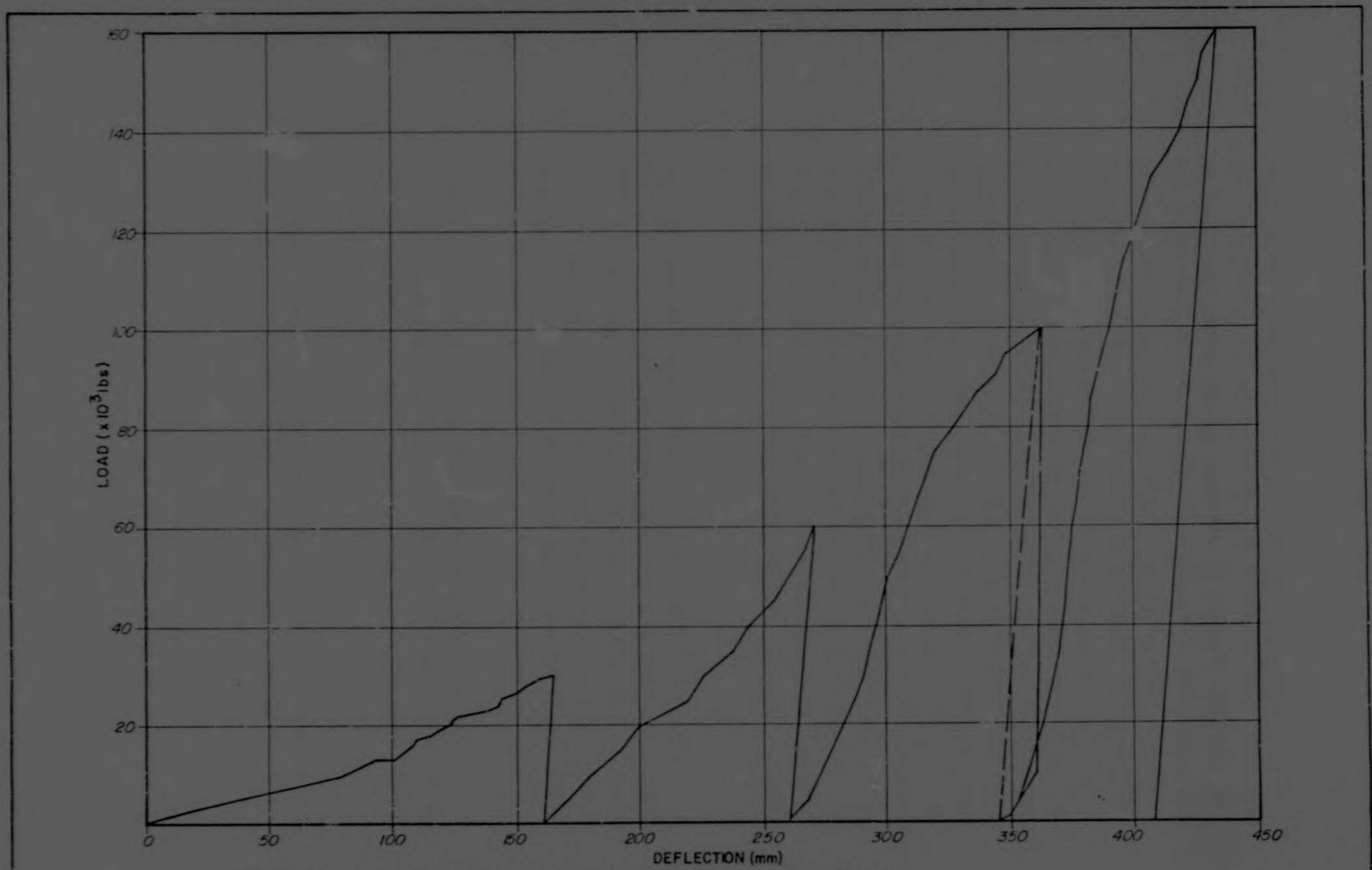


FIGURE 6.4 PLOT OF LOAD vs DEFLECTION FOR BOTH LOAD TESTS

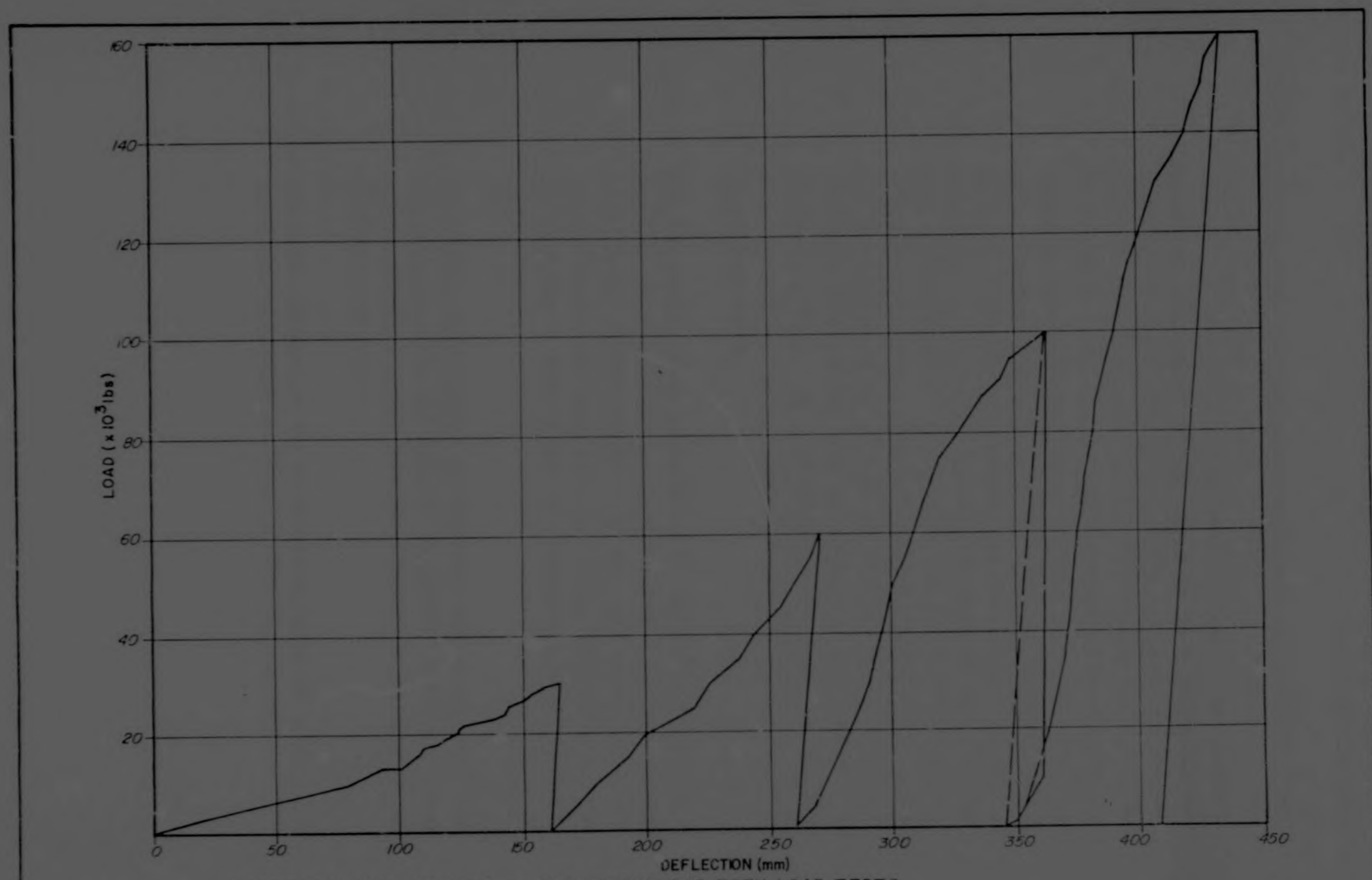


FIGURE 6.4 PLOT OF LOAD vs DEFLECTION FOR BOTH LOAD TESTS

porosity decreased substantially once the loads were applied. This is illustrated in Figure 6.3 where the deflection at the various load levels and the decrease in porosity are plotted. The direct relationship between the increase in deflection and the decrease in porosity is evident in the graph and follows from the assumption that lateral displacement is negligible when compared to the vertical displacement. To get around this (possibly erroneous) assumption in future tests, the volume of voids should be determined by measuring the amount of water required to submerge the specimen in the cylinder. Change in volume measurements could also be incorporated into the load tests by waterproofing the equipment and leading the piezometer tubes into measuring flasks or burettes. A far more accurate and meaningful set of results would therefore be obtained. This stems from the fact that the flow equation is dependent on the void volumes, ie porosities, which would be measured directly in future tests rather than derived from deflections, as was done presently.

All the loading tests performed on the specimen are plotted in Fig 6.4. In the second loading test the specimen was unloaded at 1 334 kPa (60 000 lbs) and 2 223 kPa (100 000 lbs) to insert spacers between the cross head and the top loading plate. This was necessary because of the large displacements of the specimen.

The loading curve becomes progressively steeper as larger preconsolidation loads are applied. In contrast however the slope of the unloading curve, or rebound curve, is the same at all initial stress levels.

The loads, deflections and porosities at which the various flow tests were undertaken are given in Table 6.3 overleaf.

TABLE 6.3 : DEFLECTION (AFTER REBOUND) AND POROSITIES OF SAMPLE

Test No	Load applied (kPa)	Deflection (after rebound, mm)	Porosity
1	0	0	0,490
2	667	162	0,423
3	3 556	407	0,290

If the specimen is assumed to have increased in width due to loading by penetrating the lining by 25 mm on either side (on average), the porosity of the sample for the third test increases from 0,290 to 0,388. This is a substantial change and illustrates the sensitivity of the diameter of the sample assumed or the porosity calculated.

If the change in porosity calculated here is compared to that obtained by Blight and Caldwell (1980), as shown in Fig 6.5, a fair amount of correlation is apparent. Because Blight and Caldwell used an unlined cylinder, more fracturing and packing took place near the walls resulting in lower porosities at higher loads. In the absence of any other checking procedure therefore, the porosities obtained from the deflections were used without any corrections.

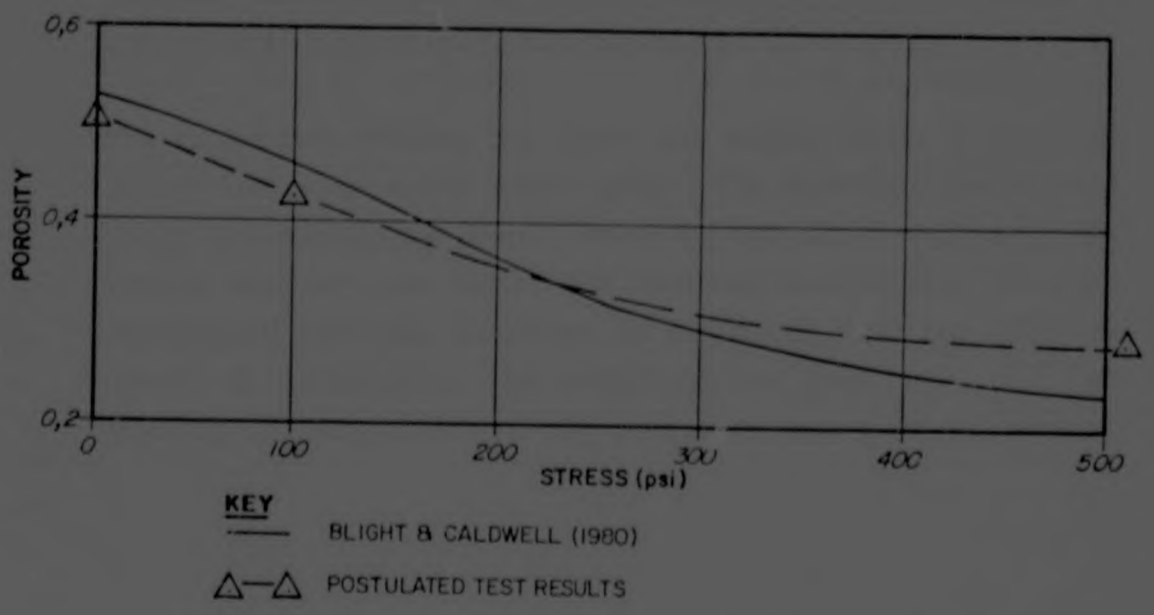


FIGURE 6.5 COMPARISON OF CHANGES IN POROSITY

6.5 Flow tests

The effective particle diameter used in the calculation of the friction factor and Reynolds number is sensitive to the type of layered model (if any) assumed in the reduction of the velocity and gradient readings. On unpacking the sample for final size analysis it was observed that the stone was crushed more in the core of the sample than near the walls. In terms of the layered flow models this would immediately suggest the use of the parallel layer model. As mentioned previously, the lining facilitated the distribution of stress throughout the height of the sample.

A greater amount of crushing near the loading platens than at the centre of the sample was not observed, substantiating the assumption of uniform stress throughout the height of the sample. If this had not been the case, the series layer model should have to been applied.

The calculated flow velocities and averages of the hydraulic gradient measured over the various distances are plotted in Figs 6.6, 6.7 and 6.8. The equations fitted to the points indicate that the flow tests were all conducted in the turbulent (partly transitional) region. This follows from the fact that the slopes of the equations are very nearly equal to 2,00. These results are also very different from those obtained by Dudgeon (1966) Fig 2.1 and used by Leps (1973), because flow is not so much transitional, but turbulent.

The difference between the first and second tests is probably within the experimental error range. The equations may be said to be essentially the same. There are two short comings in the second load and flow test: the load was insufficient to cause substantial particle breakage, as evidenced from the relative amount of deflection. The result of the first load test was probably to only rearrange the particles into a denser packing

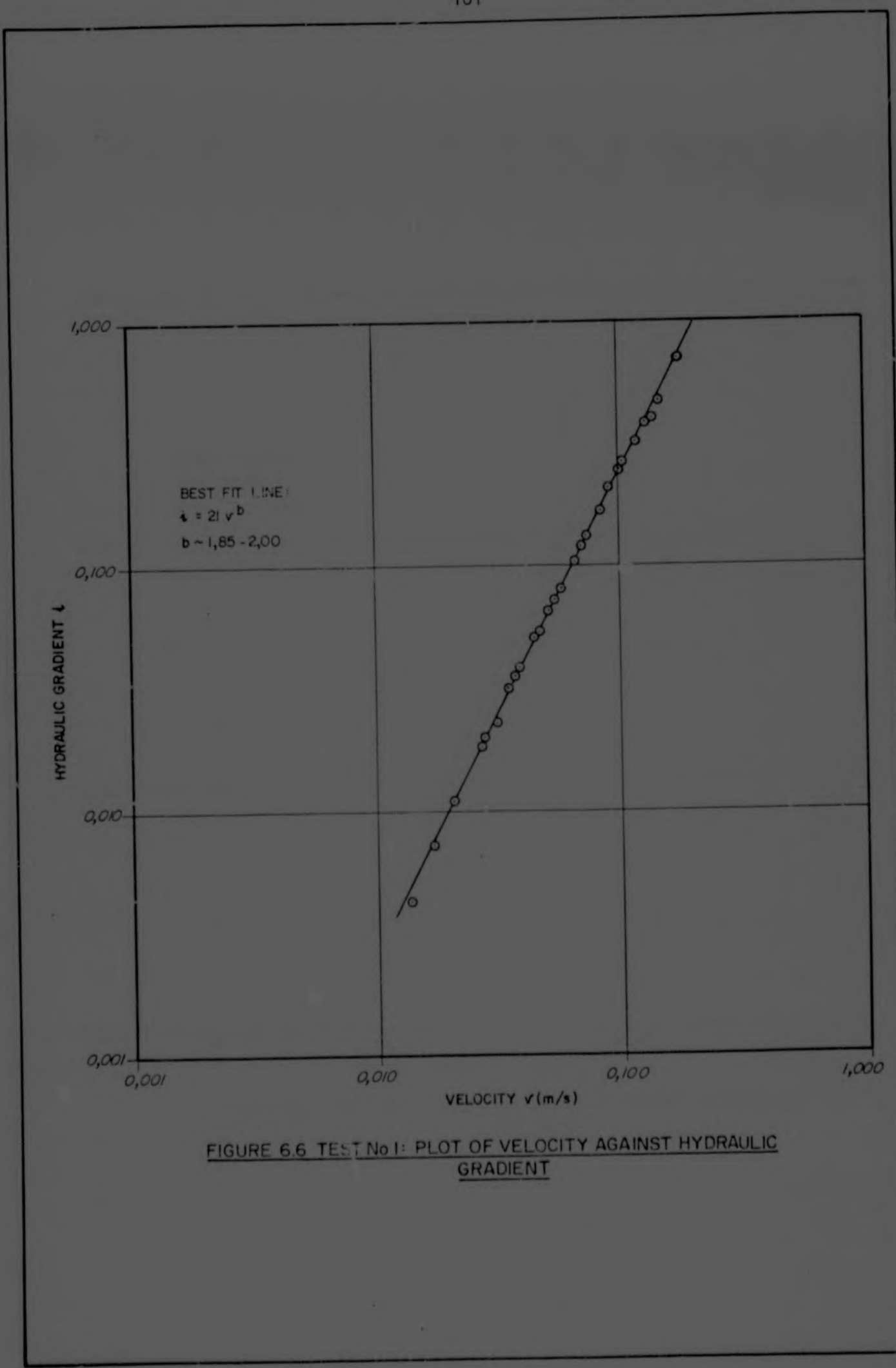


FIGURE 6.6 TEST No 1: PLOT OF VELOCITY AGAINST HYDRAULIC GRADIENT

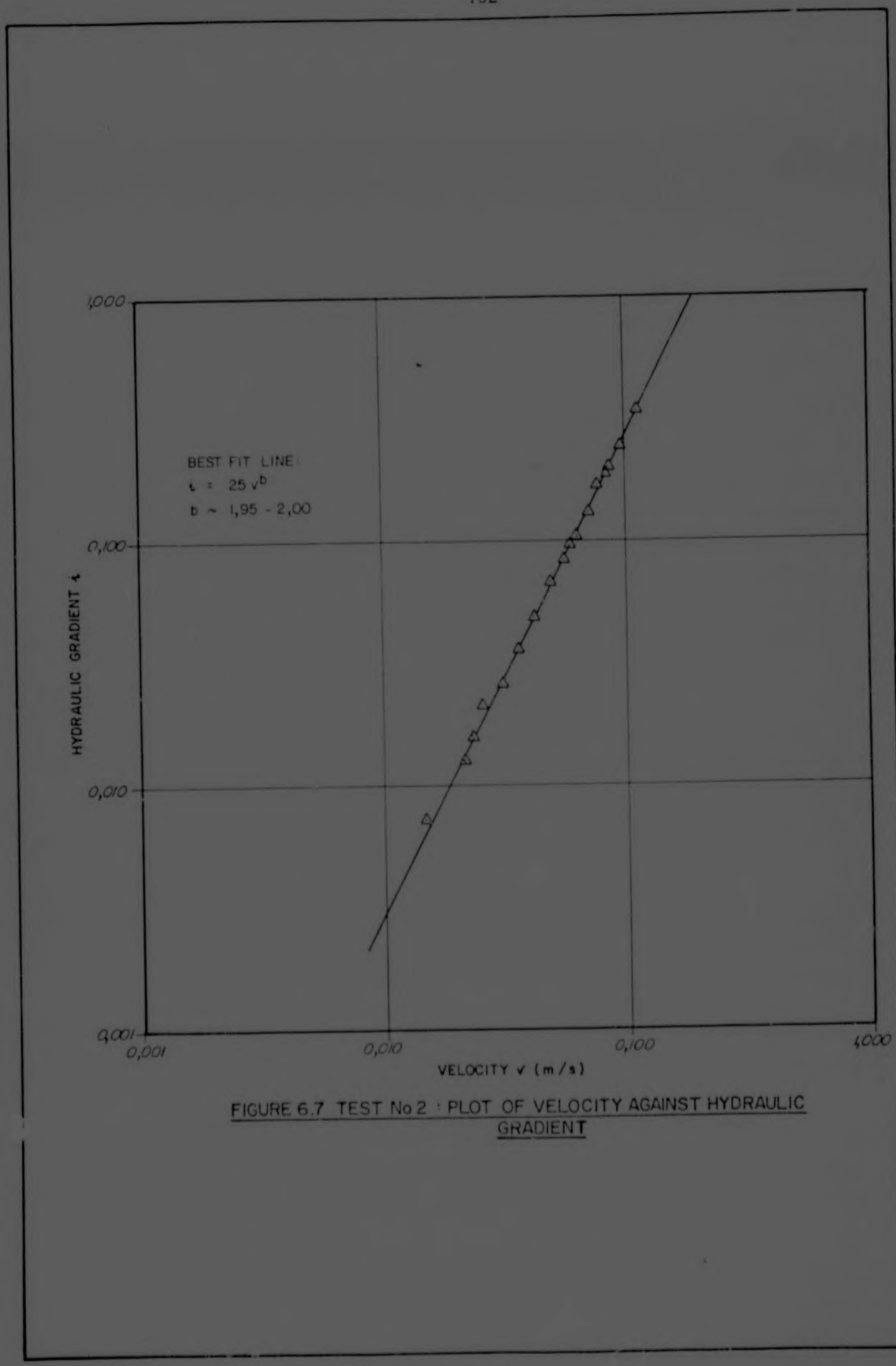


FIGURE 6.7 TEST No 2 : PLOT OF VELOCITY AGAINST HYDRAULIC GRADIENT

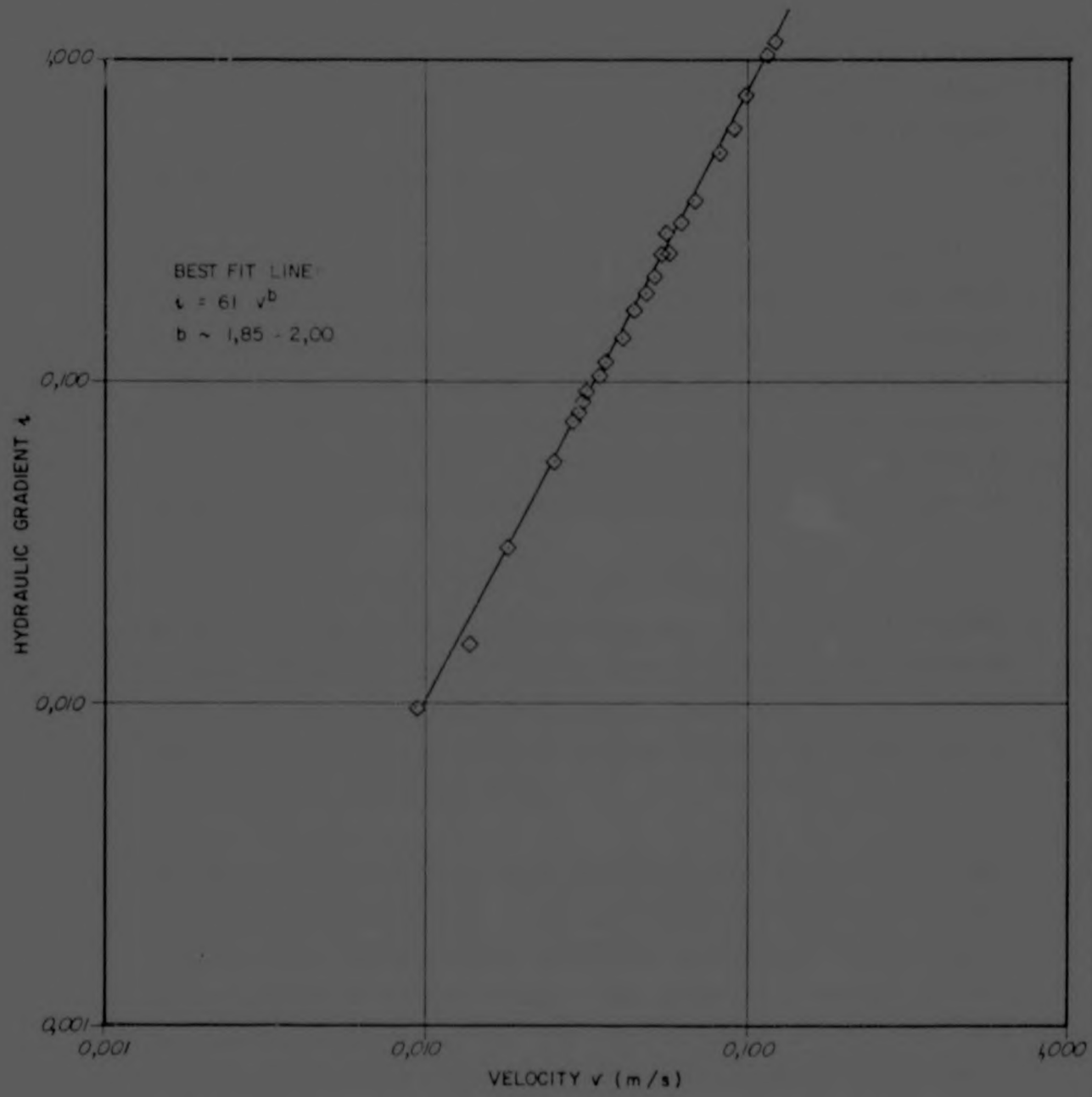


FIGURE 68 TEST No 3: PLOT OF VELOCITY AGAINST HYDRAULIC GRADIENT

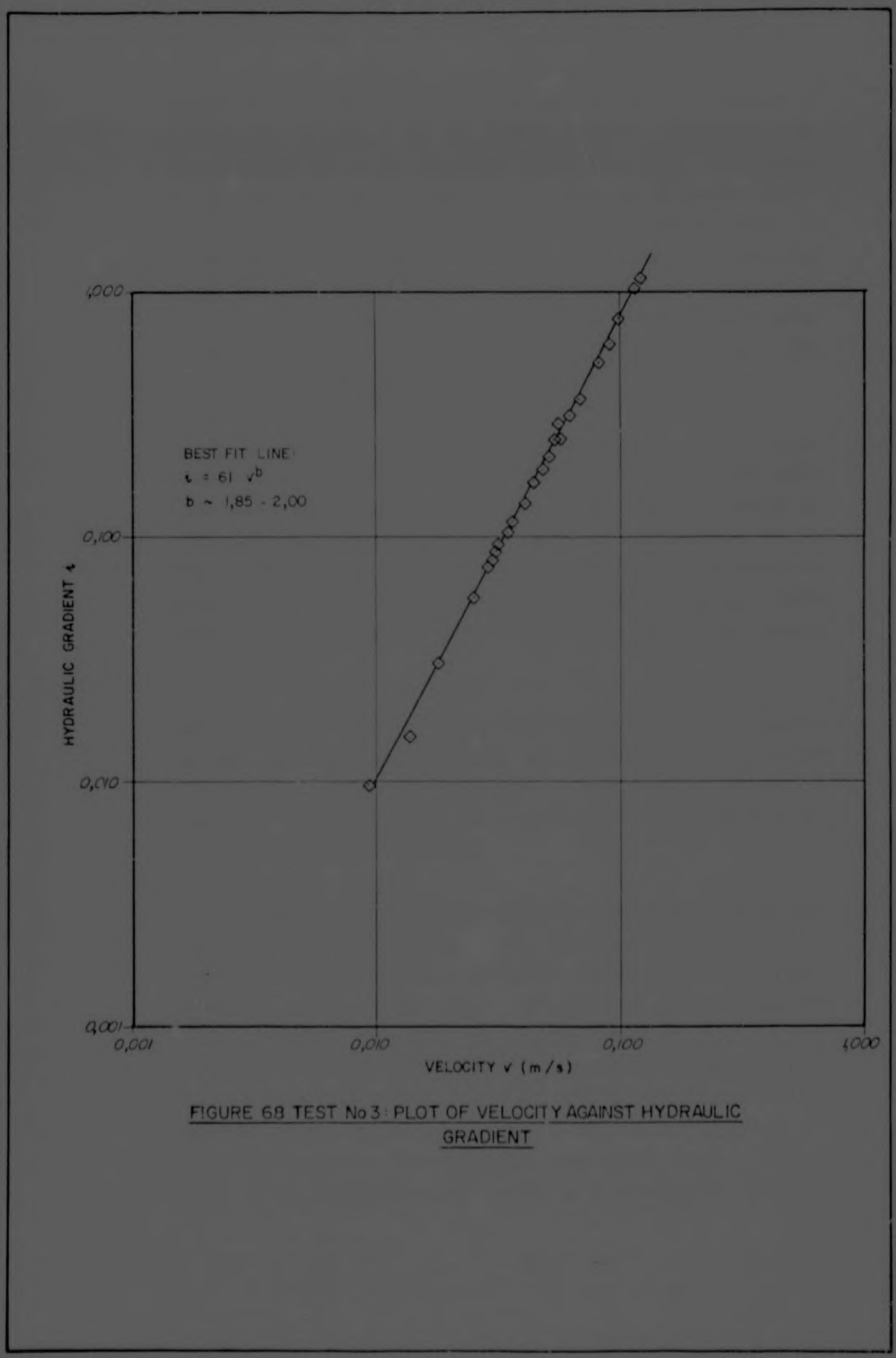


FIGURE 68 TEST No 3: PLOT OF VELOCITY AGAINST HYDRAULIC GRADIENT

coupled with limited breakage. The assumption of the change in grading may therefore not be totally correct. The sample was not unpacked and graded after the first load test. The amount of particle breakage and hence the grading and effective particle diameter were interpolated by means of Equation 2.30. A sieve analysis may also exaggerate the amount of particle breakage under load. During the flow tests the particles, although broken may still be positioned adjacent to each other in such a way as to present a similar size range of particles as far as the flow paths are concerned.

It is evident that the change in porosity has a strong influence on the permeability of the sample when the first and third flow tests are compared. The contribution due to the change in effective particle diameter can only be established if in future tests, the sample were to be "remoulded" to the original porosity after crushing. This is quite easily done by simply emptying the cylinder and then loading it to a required amount of deflection.

Because all the tests performed fell into the turbulent region, it was impossible to determine the constant C_1 of equation 2.10 with any degree of confidence. From Fig 2.3 it can be seen that K approaches C_2 at a high enough Reynolds number, regardless of the value of C_1.

An important result to emerge from the flow tests however was the fact that equation 2.10 has the same constant C_2 for samples with substantially different porosities (recall equation 2.10 is $K = C_1/R + C_2$). The plots of friction factors against Reynolds number for the various tests are given in Figs 6.9, 6.10 and 6.11. The arithmetic mean values of the friction factors vary between 4,5 and 5,4. The curves fitted to the measured points have a C_1 value of 800 on the strength of data from previous investigators, (see Table 2.1). The C_2 value is an empirical value which is a function of particle

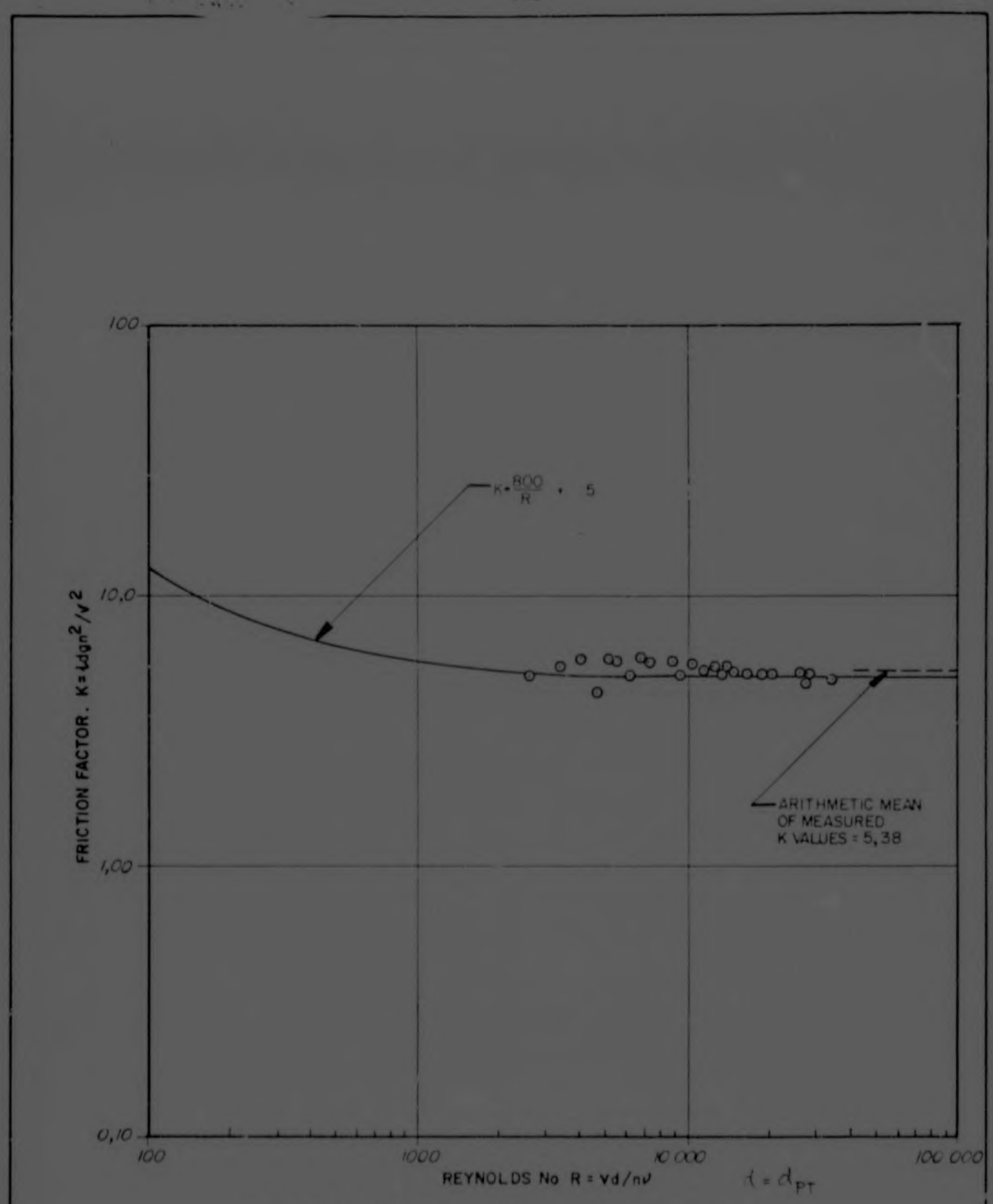


FIGURE 6.9 TEST No1 : PLOT OF FRICTION FACTORS

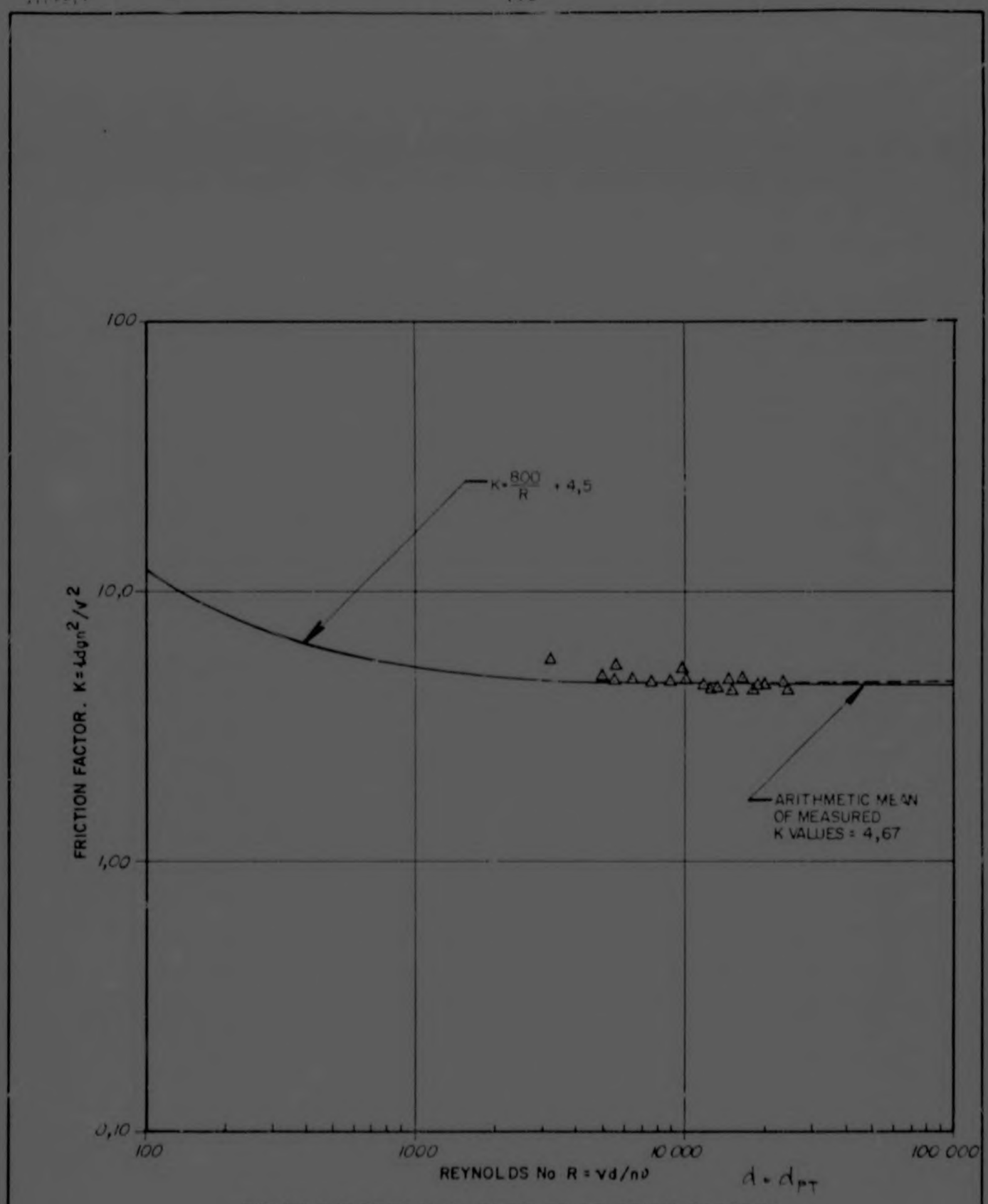


FIGURE 6.10 TEST No2: PLOT OF FRICTION FACTORS

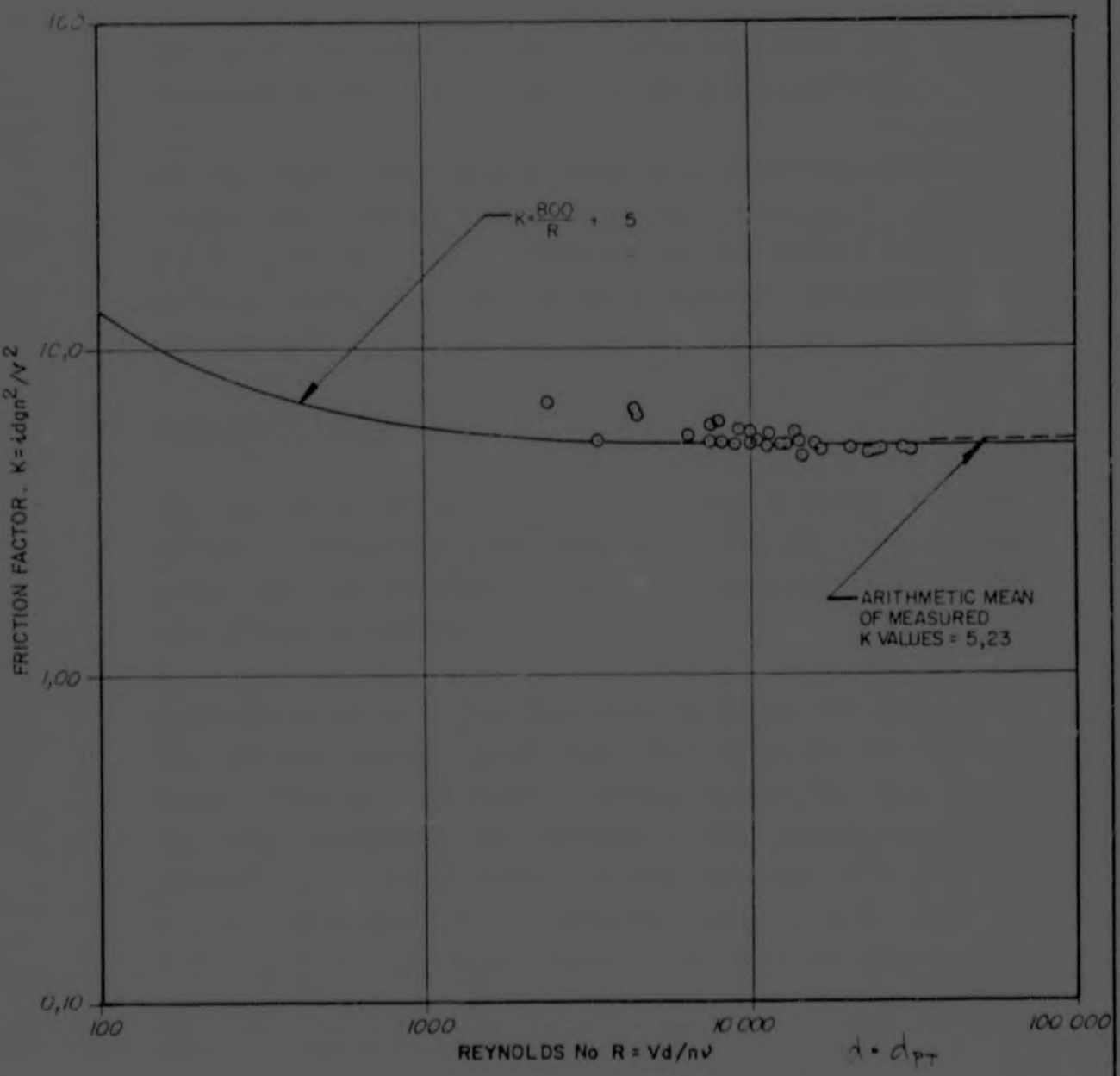


FIGURE 6.11 TEST No 3: PLOT OF FRICTION FACTORS

shape and roughness. Because of this qualitative desciption to arrive at this value, the accuracy of the C_2 value should only be taken to the first decimal point, as there is no physical meaning in a difference in C_2 values of smaller amounts. The entire range of C_2 from smooth polished marbles to rough angular rock is from 2 to 5.

The use of the friction factor - Reynolds number plot can be justified therefore on the basis of the tests performed.

The velocity-gradient graphs showed a considerable difference, whereas the friction factor plots were essentially similar. The tests did not cover all flow regimes and particle types (eg marbles, flatter stone etc) to prove universal applicability of equation 2.10.

6.6 Suitability of lining

The flow tests indicated that the lining overcame any edge effects. Piezometer tube readings inside the core of the sample were not significantly different to those taken at the wall of the permeameter.

Difficulties arose in the flow tests to define the diameter of the cylinder through which flow took place at the various loads. From the load tests it became evident that the lining was soon penetrated and pierced. The lateral restraint afforde to the sample during the load tests was negligible and a large percentage of the movement probably took place in rearranging the particles laterally as well as compressing. The lining was therefore responsible for the non-uniform pattern of particle breakage.

6.7 Conclusions

Particle size analyses were performed before loading and after the final load test. Because the sample could not be removed for size analysis after the first load test, the amount of particle breakage and hence grading were interpolated by means of equation 2.30. The load tests had the combined effect of reducing the effective particle diameter and the porosity of the sample. The change in flow characteristics is therefore as a result of a change in both these parameters.

Further changes, such as the particle shape, were not considered here, although it was observed that a large portion of broken particles were elongated.

Simplifying assumptions regarding the relationship between deflection and porosity had to be made. As mentioned previously, an improvement on the testing method would be to measure the change in the volume of voids directly. Because the specimen was hand-packed, the initial porosity was fairly high at 0,490. This decreased to 0,423 and 0,290 after the first and second loading tests.

The change in porosities in the load tests were compared to previous tests by Blight and Caldwell (1980) and accepted on that basis for further reduction of the results.

The lining in the cylinder provided a stress relief zone near the walls due to lack of restraint. Consequently the amount of particle breakage decreased from the core of the sample outwards. This was confirmed on unpacking the sample where the stone was found to be crushed more in the core than near the walls. The lining provided relatively little frictional restraint so that the specimen could be considered to be evenly stressed throughout its depth. Therefore the parallel layer model was assumed in the flow tests.

The flow tests indicated that the lining overcame any edge effects. Piezometer tube readings inside the core of the sample were not significantly different to those taken at the wall of the permeameter.

The flow tests all fell within the turbulent flow regime. This was demonstrated by plotting the hydraulic gradient against the gross flow velocity on a log-log scale. Further tests would be required in which either smaller sized particles or lower flow rates are used. (However, difficulties arise in measuring the hydraulic gradient for lower flow rates with a measureable degree of accuracy). These tests would furnish the data required to calculate the laminar friction factor C_1 in equation 2.10. Because of the turbulent flow in most of the tests only the turbulent friction factor C_2 could be evaluated with any degree of confidence.

The test results illustrate the fact that:

(i) The Forcheimer equation in its form $K = C_1/R + C_2$ provides a better means than an exponential equation of describing the flow through porous media of different particle zies and porosities, and

(ii) it is possible to predict the reduction in throughflow characteristics of a rockfill subjected to large stresses and degradation from the change in particle size and porosity, taking the layering and arrangement of particles into account.

7 GENERAL CONCLUSIONS

7.1 Literature review

The experimental results of numerous flow tests by various authors have been analysed and compared (Table 2.1). From the comparisons it can be deduced with reasonable confidence that the equation of the form:

$$K = C_1/R + C_2 \qquad \text{.....(2.10)}$$

is applicable for most practical purposes to the flow through coarse porous media. The effect of porosity and particle diameter on the flow equation needs wider investigation.

It was revealed in the literature that single sized particles, which make up a more efficient medium for drainage, degrade under load and are thus structurally inefficient and may even clog eventually. Because of the great diversity of uses to which rockfills and gravels are put, there are a number of standard desciptors and classification values by which the mechanical strength and grading may be defined. These values are important for the prediction of crushing under load. This will enable a prediction of the hydraulic properties to be made under any state of stress.

From both flow and loading consideration it became necessary to investigate methods of lining the testing cylinder with a material suitable for both the flow and loading tests.

7.2 Theoretical development of the flow equation

It was shown that the headloss equations for coarse porous media are functions of the fluid viscosity, particle shape and roughness, the porosity of the medium and an undefined representative particle diameter. To this end the headloss

equation was developed further to calculate the effective diameter for laminar, transitional and turbulent flow by means of the layered model.

The layered model was used to represent mathematically the variation of particle sizes and their effect on the porosity of the medium. Given the right circumstances, the effective diameter of a particular medium may be interpreted as being greater or less by factors of up to thousands, as illustrated in Table 3.2.

Matrix methods of applying the layered model were demonstrated. The orientation of the layers with respect to the hydraulic gradient affects the permeability of the medium (Fig 3.6). Since the variation in effective diameter is of several orders of magnitude, the orientation of the layers was chosen as the parameter to be varied randomly in modelling a random layered system. Table 3.4 contains the effective particle diameters for randomly packed gravels. The criterion chosen was the expected orientation of most of the layers (45°), which obviates the necessity of making the choice between an arithmetic or geometric mean of values covering a large range.

The work contained in Section 3 is a theoretical development of the equation which found good correlation with tests on single sized stone by previous investigators (Table 2.1). The equipment developed for the loading and flow tests also provides the opportunity to conduct tests in which the layered and random models may be verified.

7.3 Experimental procedure

The objectives of the tests performed may therefore be listed, in order of importance, as:

(i) To examine the feasibility of the newly developed equipment for the determination of the effects of heavy loads

on the through flow characteristics of rockfills and gravels;

(ii) To determine which mathematical model best describes the flow conditions in rockfills and gravels; and

(iii) To determine which physical characteristics of rockfills and gravels have a significant effect on their permeability under various loads.

7.4 Test results

The feasibility of the equipment as a means of determining the effect of loads on permeability was demonstrated. The true value of the equipment will only become known once the modifications to the equipment described in Section 7.5 are made, and more tests on different sized particles of the same material and on other materials of various sizes have been undertaken.

Specific tests will have to be designed to test the validity of the layered models. These could consist of preparing samples in which each size fraction is packed into the mould separately to physically model the stratified medium. Parallel, series and random layered models could be set up and tested against the theoretical flow equations.

The mathematical model employed in the description of flow through coarse porous media under load determines the relative importance of the different parameters.

The effect of the change in either porosity or effective particle diameter alone on the flow characteristics may be gauged from 'remoulded' samples in which the porosity is the same as in the initial sample.

Sensitivity analyses on the effect of lateral displacement of the sample on the calculation of the porosity revealed that

large errors occurred if the material were assumed to expand laterally by 25 mm on each side. This is not entirely unrealistic as it represents half the thickness of the liner.

An important result to emerge from the flow tests however was that if all the tests were plotted on a friction factor plot, they essentially fell onto the same line, despite their earlier substantial difference in the plot of gradient vs velocity. This result provided the first tangible evidence of the universal applicability of the equation of the form $K = C_1/R + C_2$ for flow through coarse porous media under load. It is recommended therefore that further tests be conducted on the same type of programme as initiated here to establish the validity of the flow equation through coarse porous media under any state of packing due to applied loads.

7.5 Design and construction of equipment

The equipment design for the tests would require a few modifications to improve the accuracy of the test results:

(i) The accuracy of the hydraulic gradient measurements will be improved if more piezometer taps are installed at elevations between the present taps. During the load tests the sample was crushed to such an extent that the top set of taps were exposed and therefore useless

(ii) More sensitive flow measurement devices will be required to measure low flow rates. This may be achieved by measuring the flow rate volumetrically.

(iii) At high flow rates pressure fluctuations due to turbulence become more predominant, making it difficult to read off both flow rates and piezometric heads. Throttling or attenuation devices may serve to reduce fluctuations to produce average readings.

(iv) The measurement of the volume of voids in the sample for the determination of the porosity should be done by means of filling the sample with water until the sample is submerged. Because the change in permeability after loading is due to both the decrease in effective particle diameter and porosity, it is important to measure both these parameters accurately.

(v) A direct measure of the decrease in voids volume would be obtained in the load tests if rubber seals were fitted to the inside of the cylinder and the specimen filled to the top with water. All but one or two piezometer taps should be sealed off. The change in voids volume can then be measured by the amount of water squeezed out of the cylinder via the open taps.

As a prototype for various and more extensive flow tests, the equipment designed performed adequately. By measuring both deflection and volume changes the loading tests may in future yield better results.

7.6 Practical considerations

In the prediction of the performance of filter drains under large embankment loads, the most difficult task remains the accurate prediction of the degree of particle breakage and of the reduction in the porosity of the medium. Results from tests by previous investigators and the flow tests conducted in the prototype tests indicate that the equation of the form $K = C_1/R + C_2$ is the best at present for describing the flow through coarse porous media. As long as the grading of the drainage material does not degenerate to such an extent as to cause blockage (see filter laws), virtually any load may be applied to a drain, and its capacity may then be recalculated to allow for the decrease in porosity and particle size.

8 REFERENCES

Ahmed, N and Sunada, D K, 1969 : Non-linear flow in porous media. Proc ASCE. J Hydr. Div. HY6,6883, Nov.

Arbhabhirama, A and Dinoy, A A, 1973 : Friction factor and Reynolds number in porous media flow. Proc. ASCE, J Hydr. Div. HY6, 9784, June

Bear, J, 1972 : Dynamics of fluids in porous media. American Elsevier, New York, 765 pp

Bertram, G E, 1973 : Field tests for compacted rockfill. In: Embankment dam engineering. Hirschfeld, R C and Poulos, S J (eds), Wiley-Interscience, New York, p 1-20.

Blight, G E and Caldwell, J A, 1980 : Mt. Tolman tailings impoundments, technical design details. Unpublished report, Tucson, Arizona.

Caldwell, J A, 1972 : Theoretical determination of the fluid potential distribution in jointed rocks. MSc thesis, University of the Witwatersrand, Johannesburg.

Cedergren, H R, 1977 : Seepage, drainage and flow nets. J. Wiley & Sons, New York.

Cnan, C K, 1969 : Strength characteristics of rockfill materials. Speciality Session No 13, 7th Int. Conf. Soil Mech. Found. Eng. Mexico.

Dudgeon, C R, 1966 : An experimental study of the flow of water through coarse porous media. Houille Blanche, No 7.

Dudgeon, C R, 1967 : Wall effects in permeameters. Proc. ASCE, J. Hydr. Div. HY5, 5433, Sept.

Hannoura, A A and McCorquodale, J A, 1978 : Air-water flow in coarse granular media. Proc. ASCE, J. Hydr. Div. HY7, 13888, July.

Jaeger, J C and Cook, N G W, 1976 : Fundamentals of rock mechanics. 2nd ed., Chapman and Hall, London.

Lee, K L, 1969 : Particle breakage during high pressure testing. Speciality Session No 13, 7th Int. Conf. Soil, Mech. Found. Eng. Mexico.

Leps, T M, 1973 : Flow through rockfill. In: Embankment dam engineering. Hirschfeld R C and Poulo S J (eds). Wiley-Interscience, New York, p 87-108.

Leslie, D D, 1969 : Relationships between shear strength, gradation and index properties of rockfill materials. Speciality Session No 13, 7th, Int. Conf. Soil. Mech. Found. Eng. Mexico.

Marsal, R J, 1969a : Contributions and discussions on mechanical properties of rockfill and gravel materials. Ibid.

Marsal, R J, 1969b : A statistical model for granular materials. Ibid.

Marsal, R J, 1973 : Mechanical properties of rockfill. In: Embankment dam engineering. Hirschfeld R C and Poulos S J (eds), Wiley-Interscience, New York, p 109-200.

Moore, W L, 1959 : Relationships between pipe resistance formulas. Proc ASCE, J Hydr. Div. HY3 1962, Mar.

Olivier, H, 1967 : Through and overflow rockfill dams. Proc. Inst. Civil Engners, London, March.

Parkin, A K, Trollope, D H and Lawson, J D, 1966 : Rockfill structures subject to water flow. Proc. ASCE J. Soil Mech. Found. Eng. Div., SM6,4973, Nov.

Rumpelt, T K and Stephenson, D, 1982 :Stratification of rockfill embankments and the effect on permeability. 14th Int. Congress on Large Dams, Q.55, R.40, Rio de Janeiro.

Silberman, E, 1965 : Discussion on Turbulent flow in porous media, by Ward, J C, Sept 1964, Proc. ASCE, J. Hydr. Div HY1, Jan.

Snow, D T, 1965 : A parallel plate model of fractured permeable media. PhD. Thesis, University of California, Berkeley, University Microfilms Inc. Ann Arbor, Mich.

Stephenson, D, 1979 : Rockfill in hydraulic engineering. Developments in Geotechnical Engineering Vol, 27, Elsevier, Amsterdam.

Taylor, W H, 1977 : Concrete technology and practice. McGraw-Hill, Syndey.

Vesic, A S, 1969 : Strength and compressibiiity of granular materials. Speciality Session No 13. 7th Int. Conf. Soil Medi. Found. Eng. Mexico.

Wagener, F von M, 1980 : The determination of dumprock properties in field tests. Course on rockfill and gabions. SA Inst. Civil Engers. Johannesburg.

Ward, J, 1964 : Turbulent flow in porous media. Proc. ASCE. J. Hydr. Div. HY5, 4019 Sept.

Webber, N, 1965 : Fluid mechanics for civil engineers. E & F Spon Ltd. London.

Wilkins, J K, 1956 : Flow of water through rockfill and its application to the design of dams. Proc. 2nd Austr. New Zeal. Soil Mech. Conf. Christchurch.

Wright, D E, 1968 : Non-linear flow through granular media. Proc. ASCE, J. Hydr. Div. HY4, 60[12] Jul.

Yalin, M S, 1971 : Theory of hydraulic models. Macmillan Press. London.

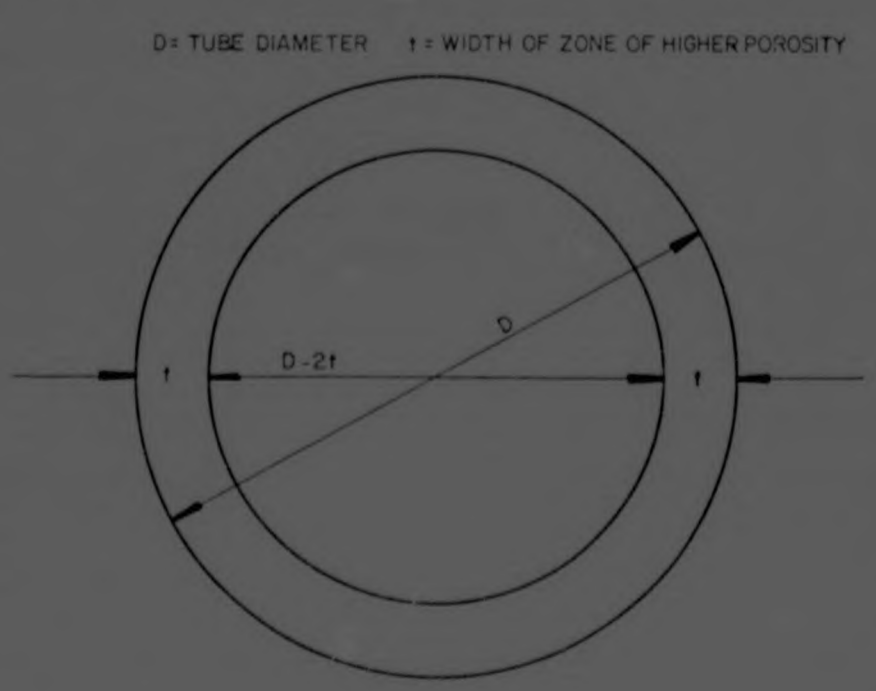
APPENDIX A

ESTIMATION OF MAGNITUDE OF WALL EFFECTS

Assuming that the presence of the perimeter wall affects the mean flow velocity mainly because of the local increase in porosity near the wall, the following simplified analysis allows the order of magnitude of the effect to be estimated. Partial input to this example is derived from Dudgeon (1967) who calculated the ratio of the mean velocity to the velocity in the inner portion of the permeameter to be 1,06 for a 16 mm gravel in a 572 mm diameter cylinder.

To get this 6% increase in velocity over the whole area as a result of an increase in velocity over the relatively small wall area means that a fairly substantial velocity increase in the wall area is required. The ratio of the velocity in the wall area to that in the inner portion of the permeameter is calculated below.

Consider a permeameter cross section as shown in Fig A.1.



A_i = INNER ZONE CROSS SECTIONAL AREA OF DIA. D-2t
A = TOTAL CROSS SECTIONAL AREA OF DIA D
$A_w = A - A_i$ = WALL ZONE AREA

FIGURE A.1 DEFINITION OF CROSS SECTIONAL AREAS IN AN UNLINED PERMEAMETER

If the local incarease in velocity near the wall is confined to the annular zone of width t, the mean velocities through the inner zone, wall zone and total area, V_i, V_w, and V_m respectively, are related as follows, (by continuity):

$$v_m = \frac{A_w v_w + A_i v_i}{A} \qquad \text{.....(A.1)}$$

Dividing through by V_i and substituting the dimenions for the areas yields:

$$\frac{v_m}{v_i} = \frac{4 v_w / v_i (Dt - t^2) + (D - 2t)^2}{D^2} \qquad \text{.....(A.2)}$$

In the example by Dudgeon (1967)

D = 572 mm

t = $d_{50}/2$ = 8 mm

$$\frac{v_m}{v_i} = 1,06$$

Substituting these values into equation A.2 and rearranging the equation results in a ratio of the velocity in the wall area to that in the inner zone of approximately 2, ie

$$\frac{v_w}{v_i} = \frac{1,06.\ 572^2 - (572 - 16)^2}{4\ (572.8 - 64)} = \underline{2,09}$$

APPENDIX B

GRIFFITH CRITERION FOR FAILURE OF BRITTLE MATERIALS APPLIED TO CYLINDERS AND SPHERES

Because of the difficulty associated with performing direct tensile tests on brittle materials a number of indirect tests, amongst these notably the Brazilian or cylinder splitting test, were developed. The Brazilian test also provides a convenient method of studying anisotropy and the failure of rock under conditions of quite complicated stresses (Jaeger and Cook, 1976).

If a circular cylinder of radius R is compressed across a diameter between concentrated line loads of W per unit axial length of the cylinder the stresses on this diameter are:

$\sigma_x = -W/\pi R$ (tension) .....(B1.a)

$\sigma_y = W\,(3R^2 + y^2)/\pi R(R^2 - y^2)$ (compression) .....(B1.b)

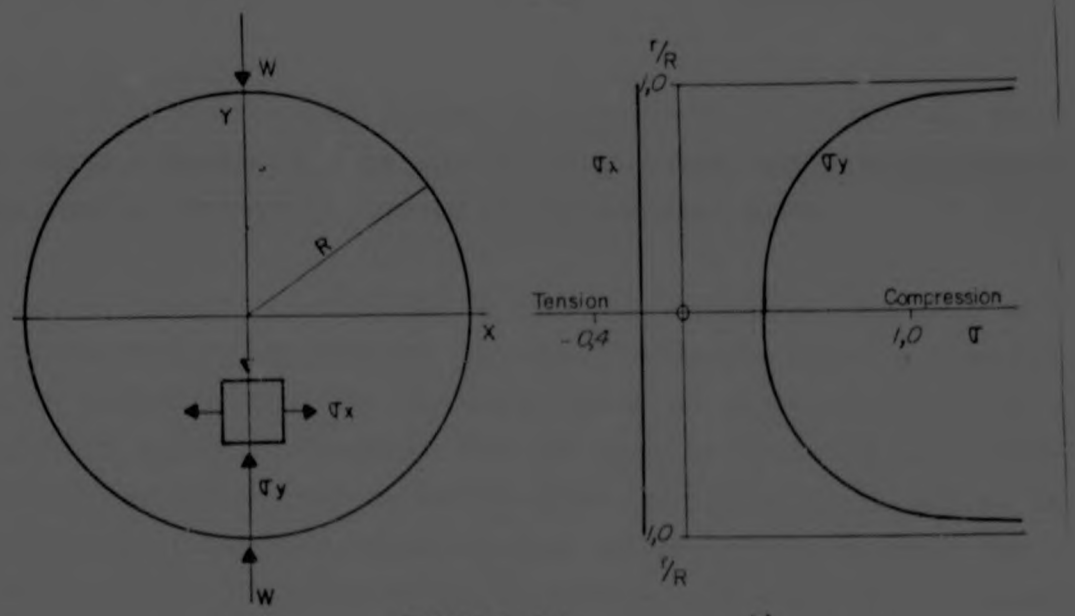
where σ_x, σ_y = stresses in the x and y directions (ie on y and x planes) respectively

On the diameter perpendicular to this the stresses are:

$\sigma_x = -W\,(R^2 - x^2)/\,(R^2 + x^2)^2/\pi R$ .....(B.2)

Equation B.2 is the general expression for σ_x at $x = 0$ in equation B.1a.

Equations B.1a and b are plotted in Figure B.1



a) FIGURE B.1 b)

CYLINDER COMPRESSED BETWEEN CONCENTRATED LINE LOADS OF W/ UNIT AXIAL LENGTH

STRESS DISTRIBUTION ON LOADED DIAMETER (Y AXIS)

When a cylinder of rock is compressed along its diameter failure occurs by an extension fracture in, or close to, the loaded diametral plane at some value of the applied load W, as shown in Figure B.2.

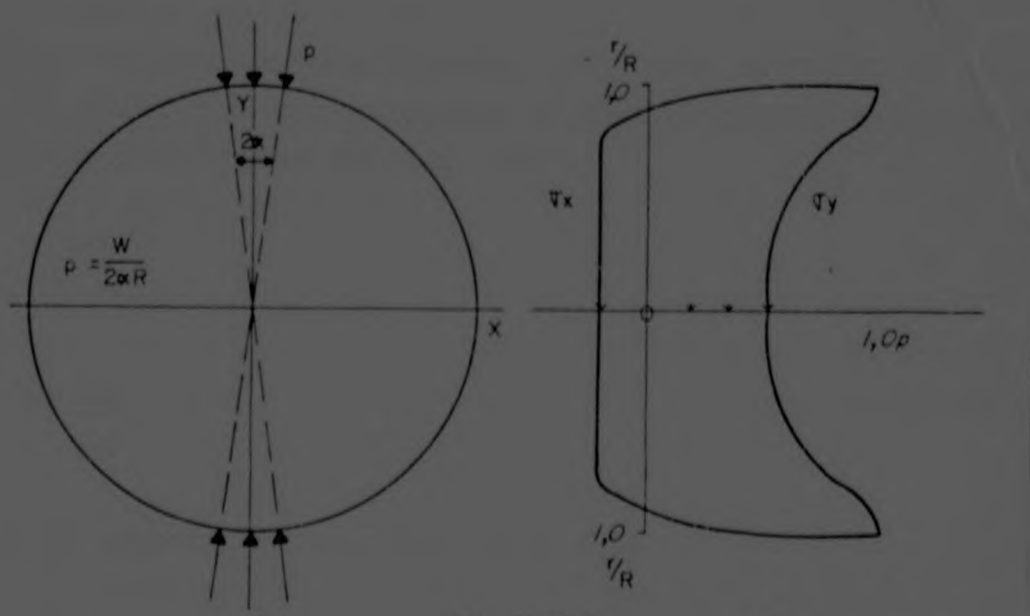


FIGURE B.2 TYPICAL FRACTURES RESULTING FROM LOADING SHOWN IN FIG B.1

It is generally assumed that failure is as a result of the uniform horizontal tensile stress σ_x from equation B.1a being equal to or exceeding the tensile strength σ_t normal to the vertical plane.

Reproducible results are obtained in this way and agree reasonably well with values obtained in uniaxial tension. Generally there are several fractures branching from the diametral plane as shown in Figure B.2, some of which appear to be wedges near the loading lines. These subsidary effects have given rise to doubts about the mechanism of failure in this and it has been suggested that failure starts by shear fracture in the region of high compressive stresses near the contact (Jaeger and Cook, 1976).

To remedy this situation, the load is ditributed over a small arc, thus reducing the maximum compressive stresses near the loading platens and thus the likelihood of shear fracture. It can be seen that the stress distribution on the loaded diameter in this case (Figure B.3) is such that the maximum compressive stresses have been reduced at the platens while the tensile stresses remain essentially the same in the body of the cylinder. Jaeger and Cook report that experiments with distributed loads over a narrow arc, usually about 15 degrees, yield tensile strength values little different from those obtained with line loads.



a) FIGURE B.3 b)

CYLINDER COMPRESSED BY DIAMETRAL LOAD p DISTRIBUTED OVER ARC 2α

STRESS DISTRIBUTION ON LOADED DIAMETER

The tensile strength determined from Equation B.1a is not the true uniaxial tensile strength, but for plane stress is determined for the principal stresses.

$\sigma_1 = 3W/\pi R, \sigma_2 = 0, \sigma_3 = -W/\pi R$ .....(B.3)

where $\sigma_1, \sigma_2, \sigma_3$ = major intermediate and minor principal stresses.

Since the ratio between uniaxial compressive and tensile strengths is seldom less than 6:1 for most brittle materials the Coulomb criterion of failure ($\sigma_1 > \sigma_c/2$ or $\sigma_1 > 6\sigma_t/2$) is rejected. From equation B.3, $\sigma_1 + 3\sigma_3 = 0$, so that in terms of the Griffith criterion, failure occurs under conditions representing the transition from:

$(\sigma_1 - \sigma_3)^2 = 8\sigma_t(\sigma_1 + \sigma_3)$

for $\sigma_1 + 3\sigma_3 > 0$

to $\sigma_3 = -\sigma_t$

for $\sigma_1 + 3\sigma_3 < 0$ .....(B.4)

which reduces to

$$\sigma_t = \frac{W}{\pi R}$$ .....(B.5)

or $$\sigma_t = \frac{2W}{\pi d}$$

where d = particle diameter

Theoretical elastic analyses extended to spheres subjected to point loads have resulted in the postulation of tensile strength equations of the following form (Jaeger and Cook, 1976).

$$\sigma_t = \frac{kW}{R^2}$$

or $$\sigma_t = \frac{4kW}{d^2}$$ .....(B.6)

where k = constant varying from 0,23 to 0,45

APPENDIX C1

SCHEDULE OF EQUIPMENT ITEMS

1 Preparation of sample

- 210 l drum plus harness
- Overhead gantry crane
- 4 000 lb spring balance
- 200 lb balance
- adjustable gauge for square or rectangular (flakiness) openings for particle size analysis

2 Flow tests

2.1 Hydraulics laboratory

- 3 kW pump
- constant head reservoir
- 205 mm N.B. delivery pipes
- valves (2)
- 150 mm sharp edged orifice + taps
- U-tube manometer, scale and mounting loard
- mercury and fluid with S.G. = 1,75
- 150 mm N.B. flexible hosing
- elbows, flange, nuts bolts etc
- sump, pvc screens
- overhead gantry crane

2.2 Cylinder

- base
- drainge valve
- gasket between base and cylinder
- male connectors for mechanical couplings on the pvc flexible piezometer hoses - holes drilled and tapped in cylinder wall

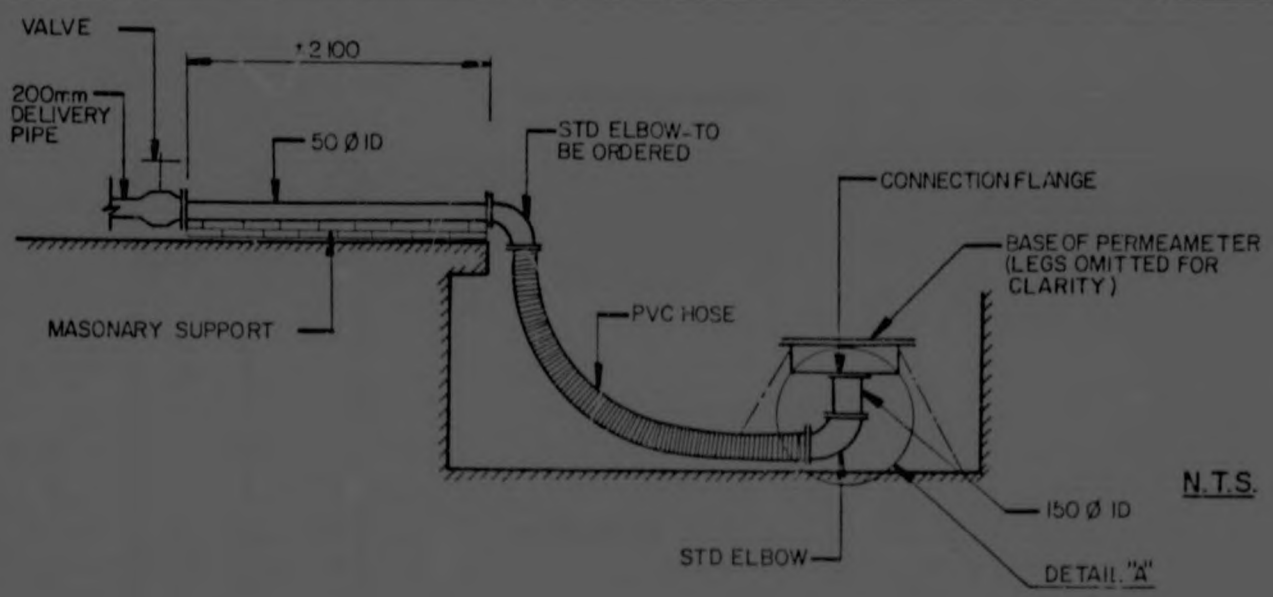
- chipblock high density foam liner
- high load industrial floor grid and supporting strip to provide base for suspended sample
- lifting yoke

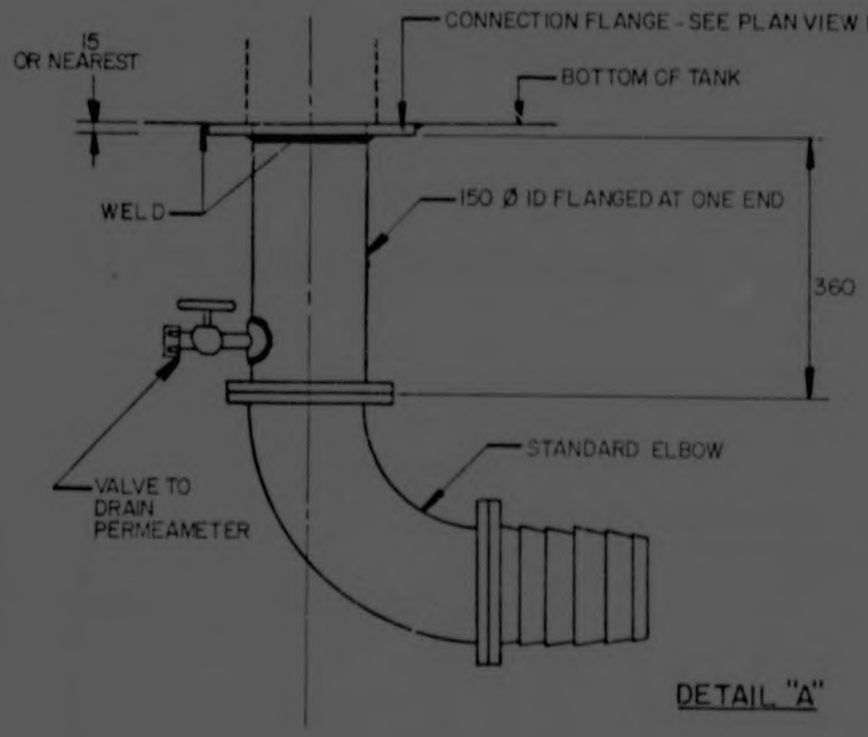
2.3 Piezometer bank

- 12 x 11 m x 6 mm nominal diameter flexible clear pvc tubing
- 3 m steel tape
- plexiglass rule and slide
- melamine coated chipboard backing
- syringe (to remove air bubbles in tubes)

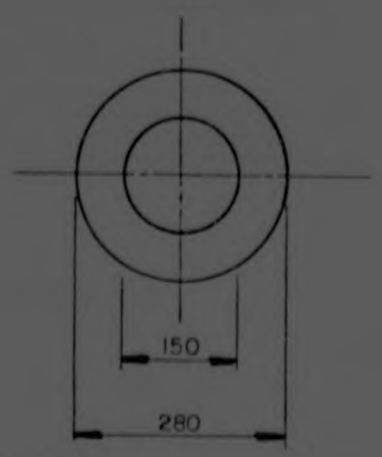
3 Loading tests

- 0,65 m wide x 3,5 m high Macklow-Smith hydraulic press capable of applying up to 170 000 pounds force on the sample
- loading plate
- pedestal supporting screen and sample
- lifting harness
- 2 t chain block
- overhead gantry crane
- dial deflection gauge





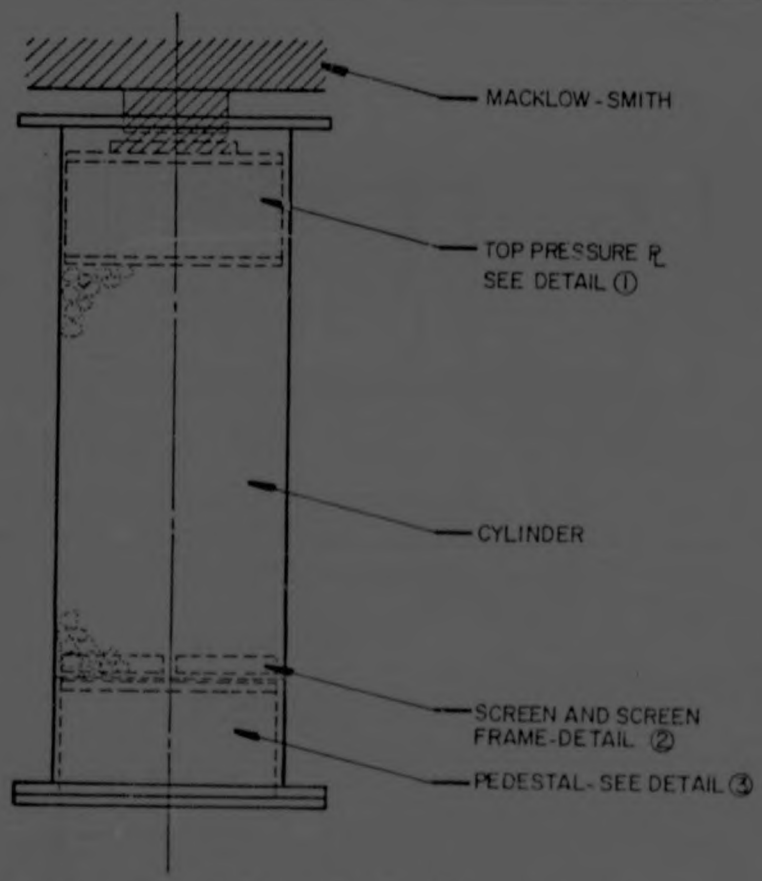
DETAIL "A"



CONNECTION FLANGE 15mm THICK (OR NEAREST)

FIG C.1

LABORATORY INVESTIGATIONAL PROJECT : T. K. RUMPELT	LAYOUT OF PIPES TO PERMEAMETER	1



ELEVATION ON PERMEAMETER IN LOADING R'G

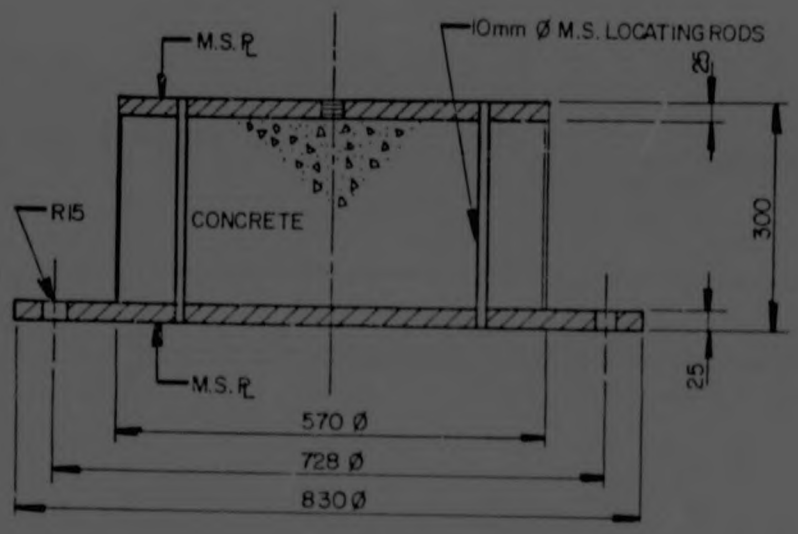
SECTION A-A

PLAN VIEW

DETAIL ①

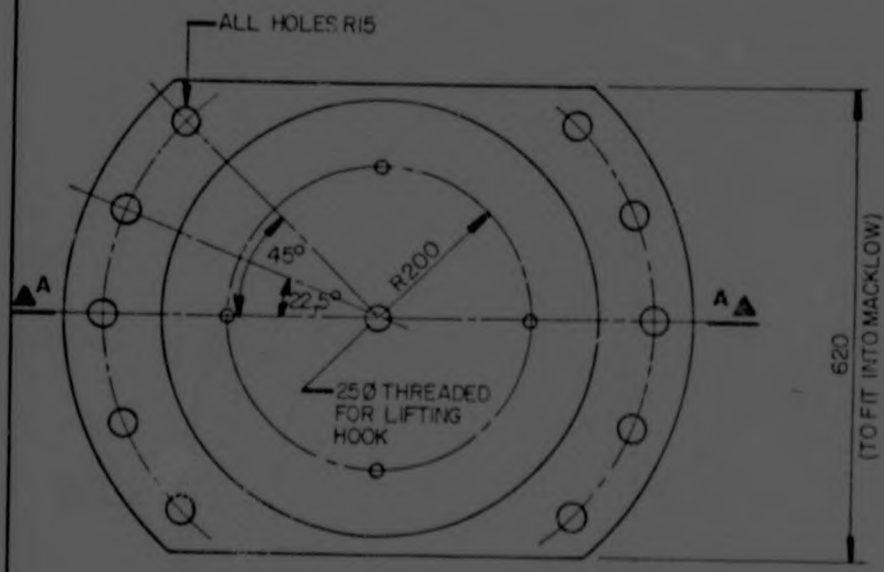
FIG C .2

LABORATORY INVESTIGATIONAL PROJECT : T. K. RUMPELT	DETAILS OF LOADING PLATES & PEDESTAL	2/1

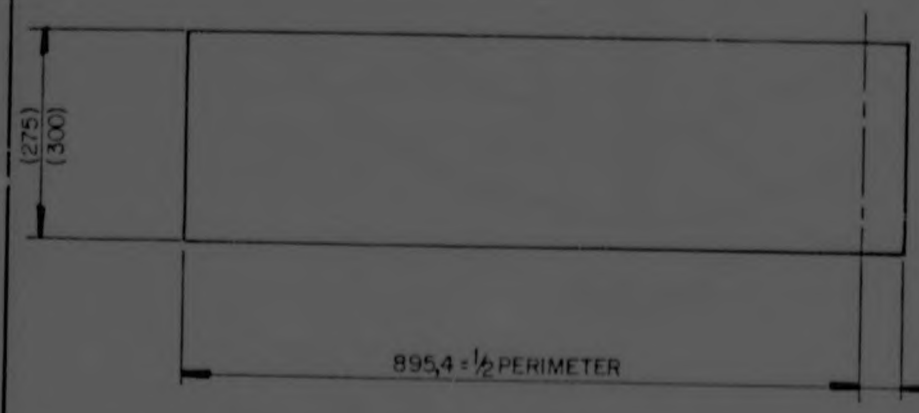


SECTION A-A

DETAIL ③



PLAN VIEW

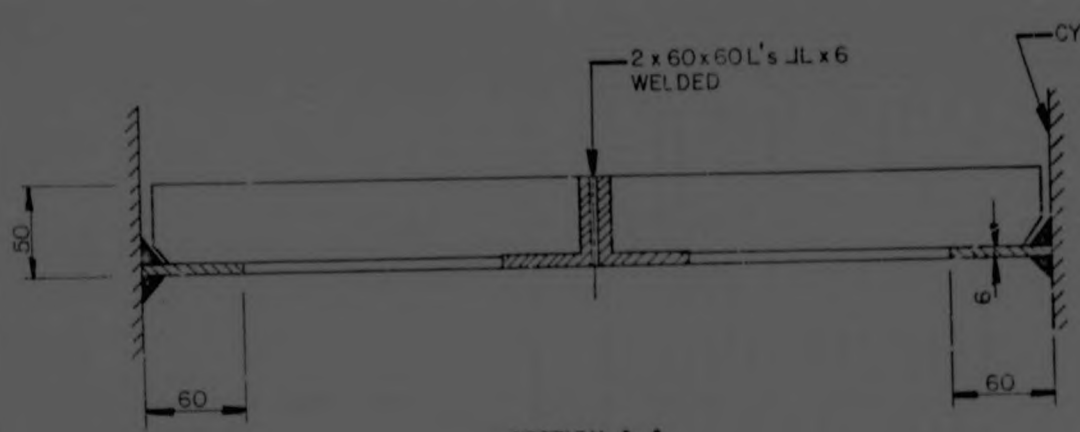


SHEET METAL DEVELOPMENT
RADIUS = 285
4 OFF : 2 x 275
2 x 300

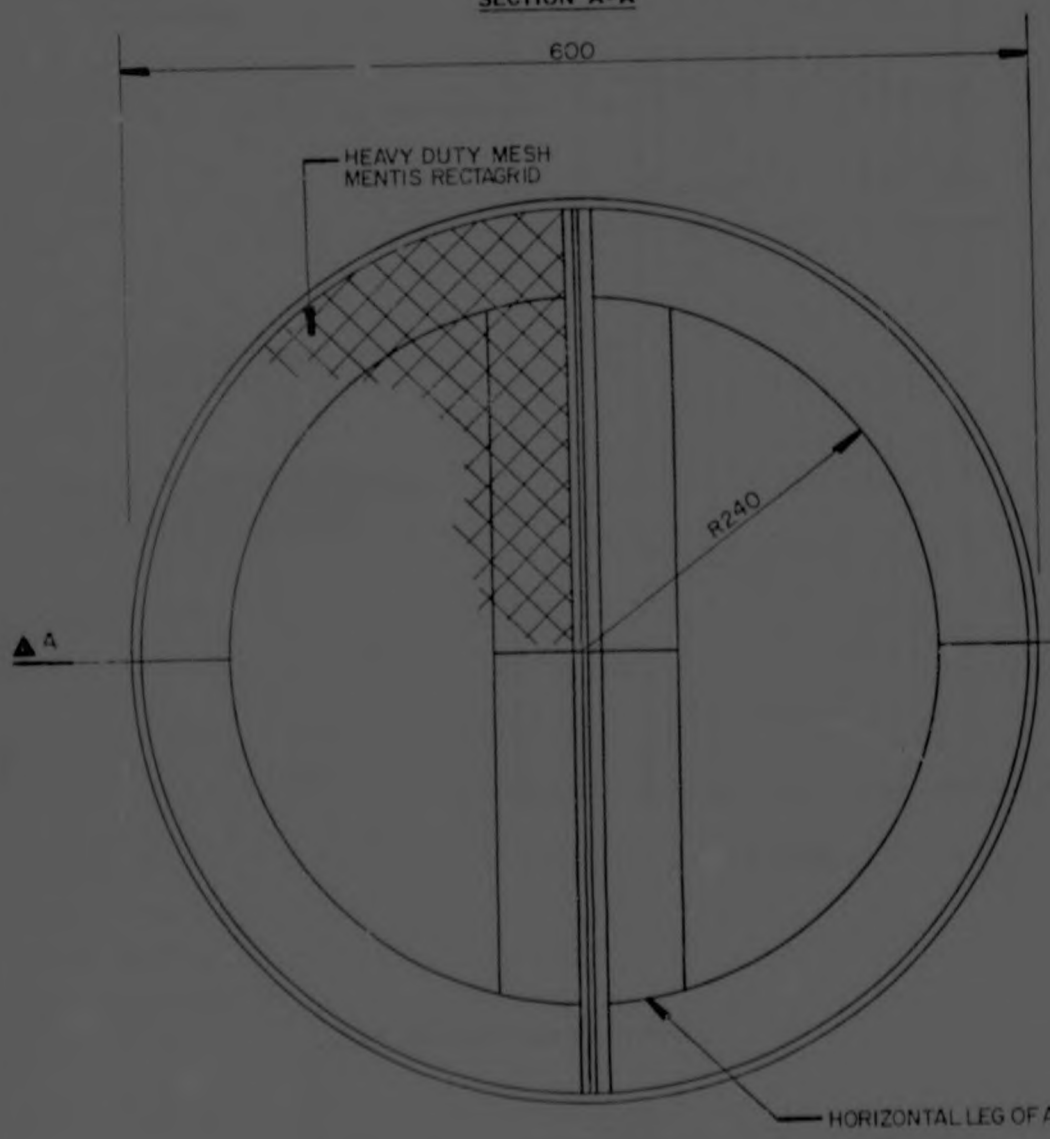
25 TO ACCOMODATE POP RIVETS OR OTHER MEANS OF CONNECTION

FIG C.3

LABORATORY INVESTIGATIONAL PROJECT : T. K. RUMPELT	DETAILS OF LOADING PLATES & PEDESTAL	2/2



SECTION A-A

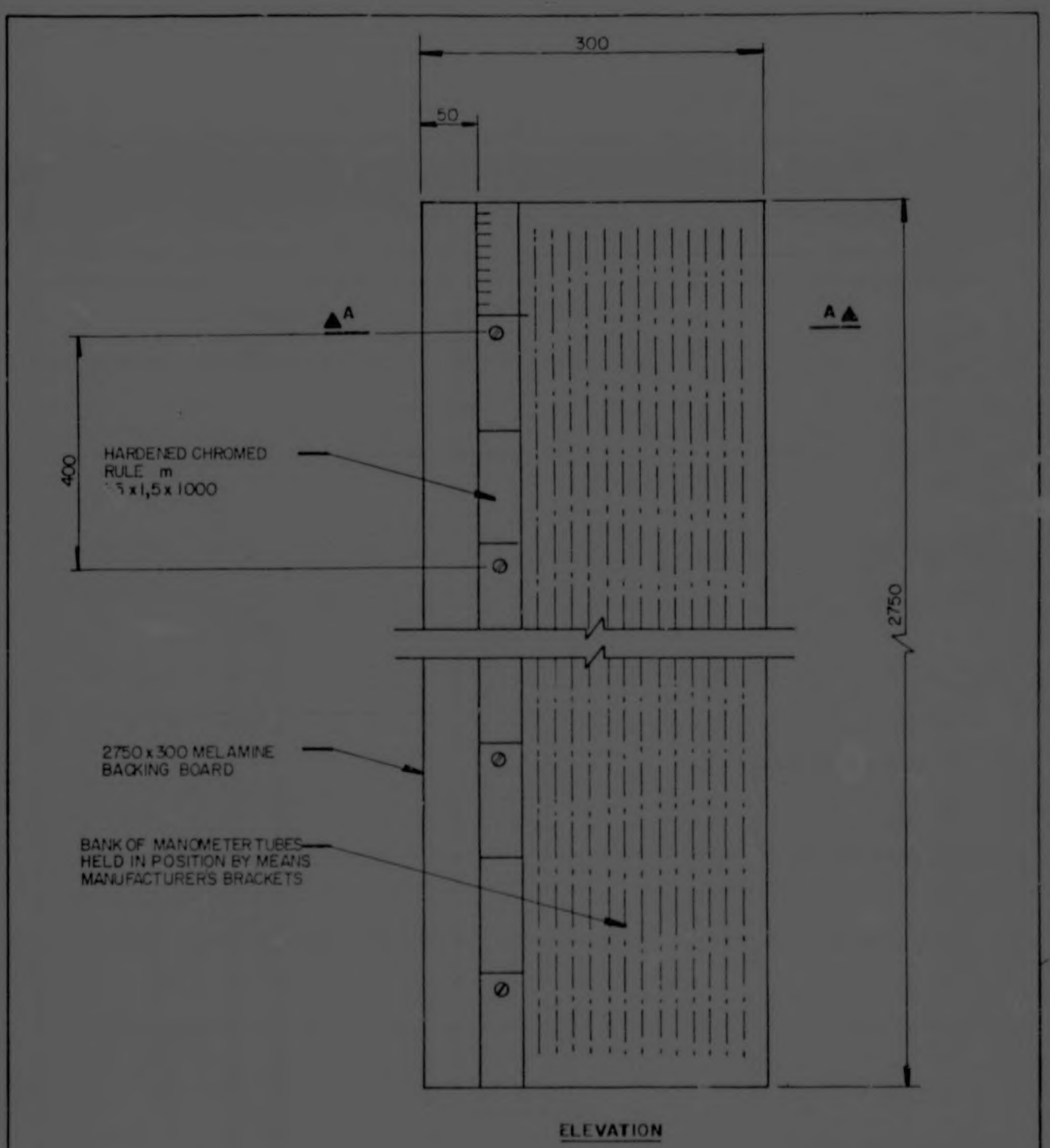


PLAN VIEW

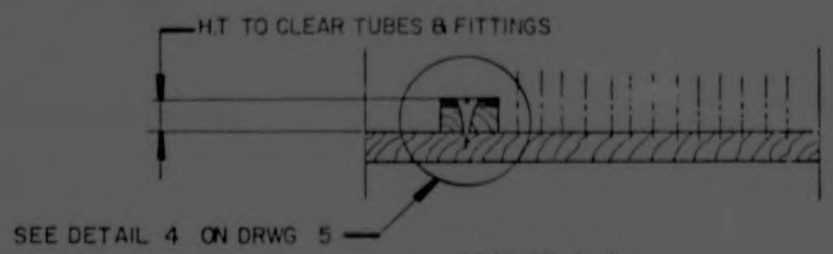
DETAIL 2

FIG C.4

LABORATORY INVESTIGATIONAL PROJECT : T.K. RUMPELT	DETAIL OF SCREEN AND SUPPORTING FRAME	3



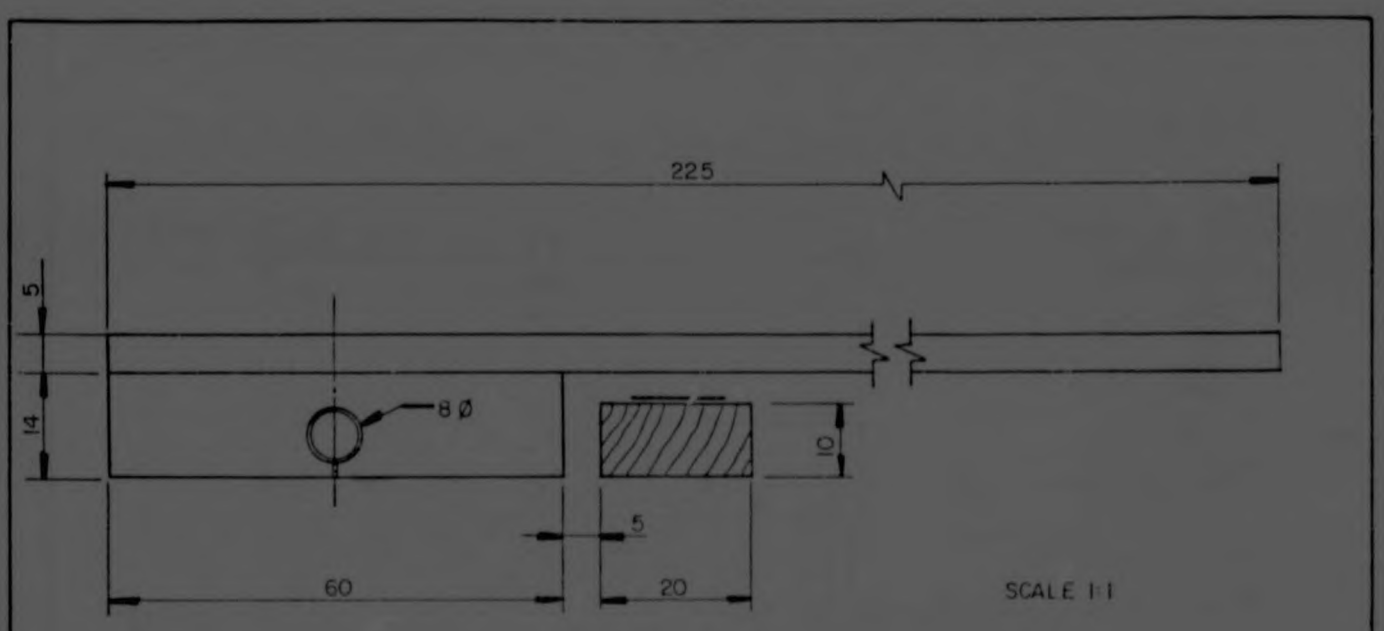
ELEVATION



SECTION A-A

FIG C.5

LABORATORY INVESTIGATIONAL PROJECT : T. K. RUMPELT	MANOMETER BOARD & FITTINGS	4



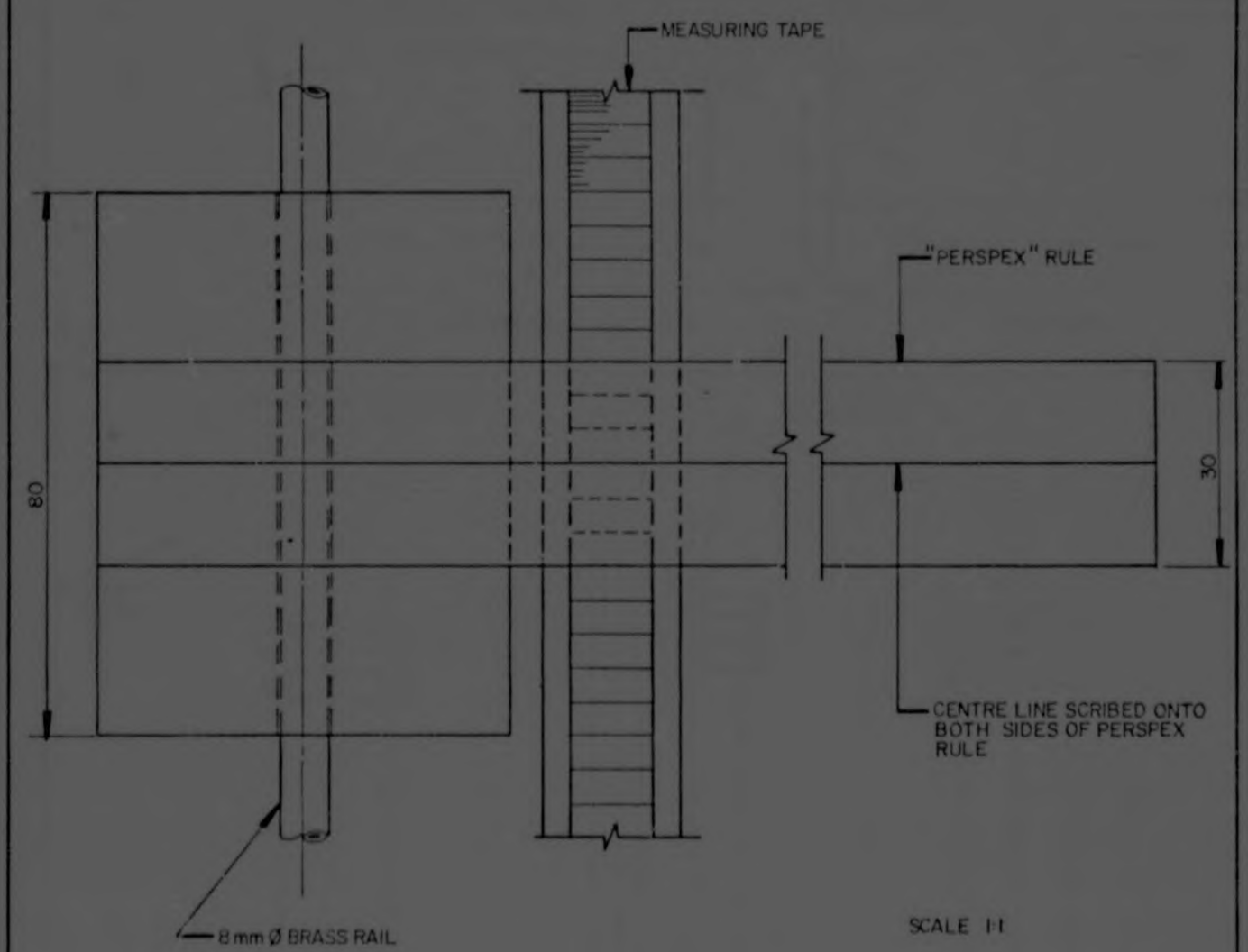
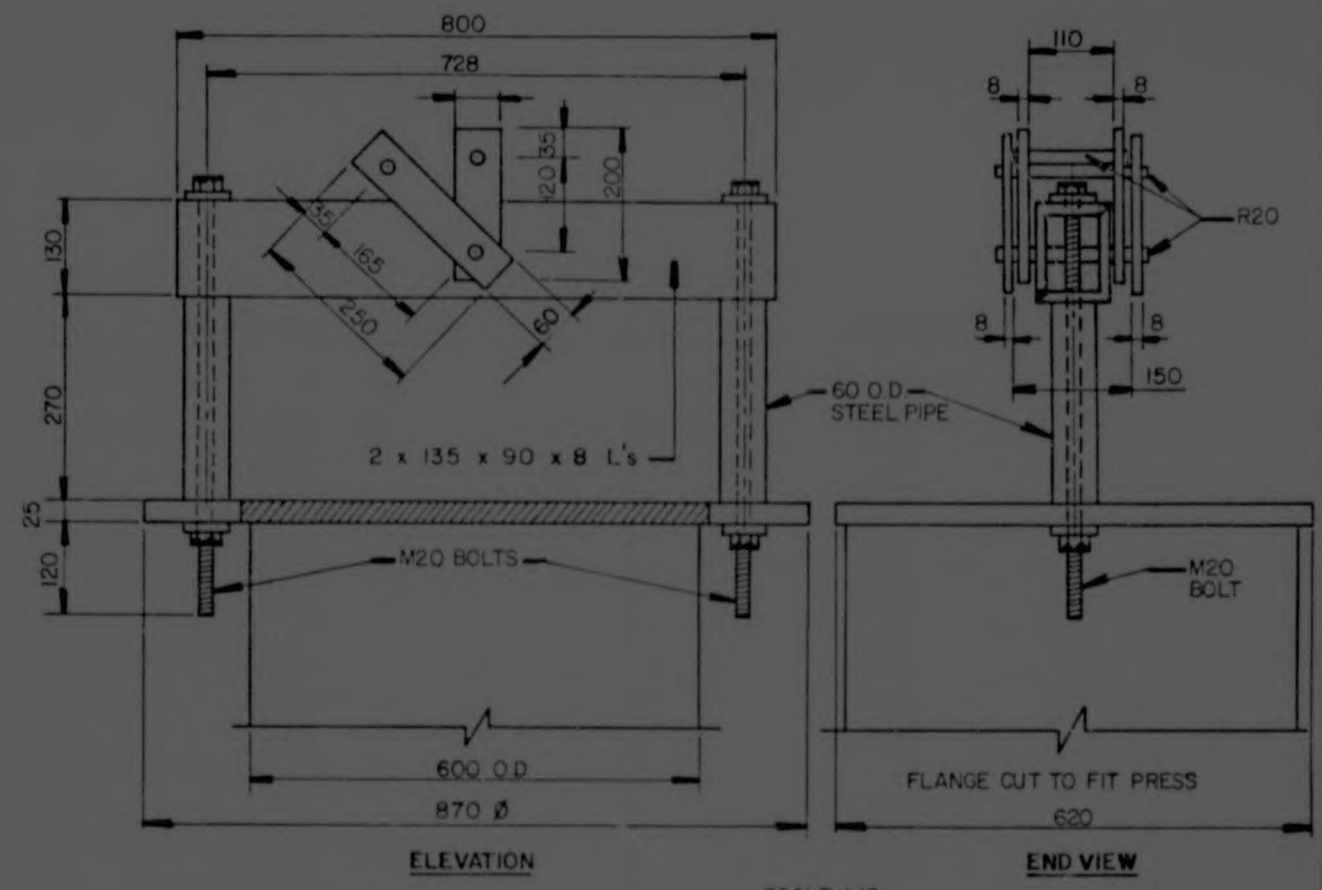
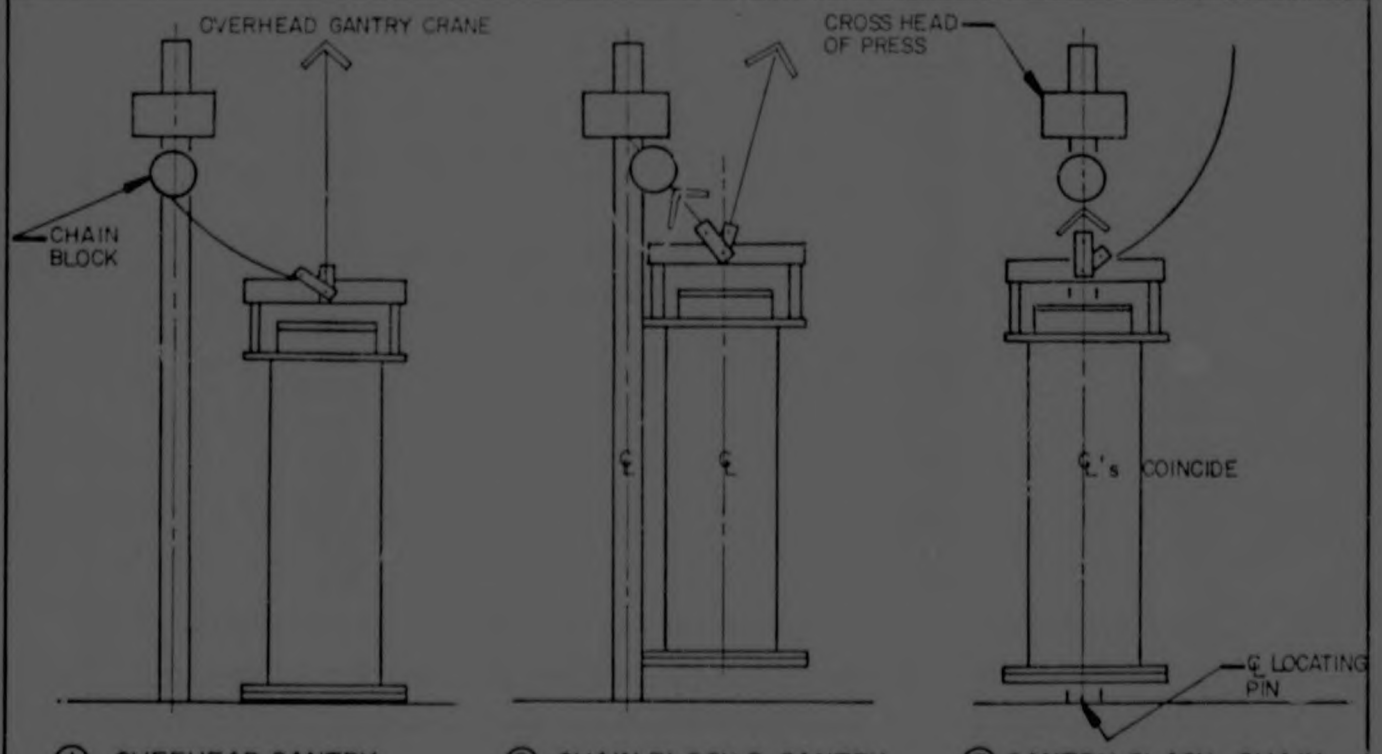


FIG C.6

LABORATORY INVESTIGATIONAL PROJECT: T. K. RUMPELT	TEE SQUARE FOR MANOMETER BOARD	5

FIG C.7





① OVERHEAD GANTRY LIFTS APPARATUS

② CHAIN BLOCK & GANTRY LIFT SIMULTANEOUSLY

③ GANTRY SLACK, CHAIN BLOCK FOR CENTERING

LABORATORY INVESTIGATIONAL PROJECT : T. K. RUMPELT	DETAILS & APPLICATION OF LIFTING HARNESS AT MACKLOW-SMITH PRESS	6

APPENDIX D1

CALIBRATION OF SPRING BALANCE

Date: 13.11.1980

Dead Wt. applied	Readings
0	20
600	655
1200	1265
1800	1890
2400	2470
3000	3020
3600	3600
3000	3040
2400	2475
1800	1890
1200	1270
600	600
0	20
600	660
1200	1275
1800	1895
2400	2480
3000	3040
3600	3610
3000	3040
2400	2480
1800	1900
1200	1275
600	655
0	20
600	655
1200	1275
1800	1900
2400	2480
3000	3040
3600	3620
3000	3040
2400	2480
1800	1900
1200	1275
600	655

LABORATORY INVESTIGATIONAL PROJECT T K RUMPELT	CALIBRATION OF 4 000 lb SPRING BALANCE C.T.1

APPENDIX D2

CALIBRATION OF ORIFICE & MANOMETER

For the range in flows during the tests, mercury was found to be not sensitive enough for the measurement of head difference in the manometer. Instead a blue fluid with a specific gravity of 1,75 was used, since water on its own would have been difficult to use (would have needed open, rather than u tube manometer).

The modified orifice flow equation, where the difference in head is measured in terms of millimetres of fluid of density ρm, is:

$$Q = C_D \sqrt{2g \frac{(\rho m - \rho w)}{\rho w} H} \qquad (D.1)$$

Where

Q = flow rate

C_D = coefficient of discharge = C k

$h = \frac{a_1 \quad a_o}{a_1^2 - A_o^2}$

a_o = area of orifice (150 mm dia)

a_1 = area of pipe (205 mm dia)

C = coefficient calculated from calibration tests

g = gravitational constant = 9,81 m/S^2

ρm = density of measuring fluid

ρw = density of water

H = difference in head measured in millimetres of fluid with density ρm

In the calibration tests Q, the flow rate, was measured volumetrically so that the above equation D.1 was rearranged to:

$$C = \frac{1}{k\sqrt{2.g.\ 0,75}} \cdot \frac{Q}{H^{\frac{1}{2}}} \qquad (D.2)$$

for $\rho m = 1,75$

A linear least squares regression analysis of the values obtained for Q yielded a value for C of 0,627 which is very close to the theoretical value.

(The regression was performed on the equation $y = a + bx$

where $y = Q$

and $x = H^{\frac{1}{2}}$)

The analysis yielded a correlation factor of 0,998 for the expression.

$$Q = -1,29.10^{-1} + 1,6277\ H^{\frac{1}{2}}$$

which returns Q in litres per second for H entered in millimetres.

APPENDIX E

HP41C LISTINGS OF PROGRAMS TO CALCULATE EFFECTIVE PARTICLE DIAMETERS AND LAMINAR, TRANSITIONAL AND TURBULENT FLOW EQUATION

E.1 Calculation of d_{PL}

```
1  LBL T PL
2  Ø
3  STO Ø2
4  LBL Ø1
5  999
6  ENTER
7  TD = ? or 999 (in mm)
8  PROMPT
9  X = Y ?
10 GO TO Ø2
11 1 E3
12 /
13 X  2
14 TX = ?
15 PROMPT
16 '
17 ST + Ø2
18 GTO Ø1
19 LBL Ø2
20 RCL Ø2
21 SQRT
22 1E3
23 *
24 TDPL =
25 XEQ t BBB
26 END
```

SUBROUTINE BBB

```
(LBL TBBB
ARCL X
AVIEW
R/S
RTN)
```

E.2 Calculation of d_{SL}

```
1  LBL T SL
2  Ø
3  STO Ø2
4  LBL Ø1
5  999
6  ENTER
7  TD = ? or 999
8  PROMPT
9  X = Y?
10 GTO Ø2
11 1E3
12 /
13 X  2
14 1/X
15 T X = ?
16 PROMPT
17 *
18 ST + Ø2
19 GTO Ø1
20 LBL Ø2
21 RCL Ø2
22 SQRT
23 1/X
24 1E3
25 *
26 T DSL =
27 XEQ T BBB
28 END
```

E.3 Calculation of d_{PT}

```
1  LBL T PT
2  Ø
3  STO Ø2
4  LBL Ø1
5  999
6  ENTER
7  TD =? or 999
8  PROMPT
9  X = Y ?
10 GTO Ø2
11 1E3
12 /
13 SQRT
14 TX = ?
15 PROMPT
16 *
17 ST + Ø2
18 GTO Ø1
19 LBL Ø2
20 RCL Ø2
21 X  2
22 1E3
23 *
24 TDPT =
25 XEQ T BBB
26 END
```

E.4 Calculation of d_{ST}

```
1  LBL T ST
2  Ø
3  STO Ø2
4  LBL Ø1
5  999
6  ENTER
7  TD =? or 999
8  PROMPT
9  X = Y?
10 GTO Ø2
11 1E3
12 /
13 1/X
14 TX = ?
15 PROMPT
16 *
17 ST + Ø2
18 GTO Ø1
19 LBL Ø2
20 RCL Ø2
21 1/X
22 1E3
23 *
24 TDST =
25 XEQ T BBB
26 END
```

E.5 Calculation of d_{PR}

```
1  LBL T PR
2  TC2 = ?  GEN = 4
3  PROMPT
4  4
5  *
6  TI = ?
7  PROMPT
8  *
9  9,81
10 *
11 1, Ø5E - 6
12 X  2
13 /
14 C1 = ?  GEN = 8ØØ
15 PROMPT
16 X  2
17 /
18 STO Ø3
19 Ø
20 STO Ø2
21 LBL Ø1
22 999
23 ENTER
24 TD = ? or 999
25 PROMPT
26 X = Y?
27 GTO Ø2
28 1E3
29 /
30 STO Ø4
31 3
32 Y  X
33 RCL Ø3
34 *
35 1
36 +
37 SQRT
38 1
39 -
40 RCL Ø4
41 /
42 TX = ?
43 PROMPT
44 *
45 ST + Ø2
46 GTO Ø1
47 LBL Ø2
48 RCL Ø2
49 TRHS =
50 XEQ T BBB
51 LBL Ø3
52 TTRIAL D = ?
53 PROMPT
54 1E3
55 /
56 STO Ø4
57 3
58 Y  X
59 RCL Ø3
60 *
61 1
62 +
63 SQRT
64 1
65 -
66 RCL Ø4
67 /
68 STO Ø1
69 RCL Ø2
70 -
71 RCL Ø1
72 /
73 100
74 *
75 T%CH =
76 XE+ T BBB
77 2
78 ENTER
79 TOK = 1,
     NOT = 2
80 PROMPT
81 X = Y?
82 GTO Ø3
83 RCL Ø4
84 1E3
85 *
86 TDPR =
87 XEQ T BBB
88 END
```

E.6 Calculation of d_{SR}

```
1  LBL T SR
3  STO Ø2
4  LBL Ø1
5  999
6  ENTER
7  D = ? or 999
8  PROMPT
9  X = Y?
10 GTO Ø2
11 1E3
12 /
13 STO Ø4
14 1
15 +
16 RCL Ø4
17 X  2
18 /
19 TX = ?
20 PROMPT
21 *
22 ST + Ø2
23 GTO Ø1
24 LBL Ø2
25 RCL Ø2
26 1/X
27 STO Ø2
28 X  2
29 RCL Ø2
30 4
31 *
32 +
33 SQRT
34 RCL Ø2
35 +
36  2
38 1E3
39 *
40 TDSR =
41 XEQT BBB
42  END
```

E.7 Calculation of laminar, transitional and turbulent flow velocity (refer to equations 2.23b, 3.b and 2.26 respectively)

```
1  LBL T VEL
2  LBL Ø1
3  TC1 = ?  GEN = 800
4  PROMPT
5  STO Ø1
6  TC2 = ?  GEN = 4
7  PROMPT
8  STO Ø2
9  LBL Ø2
10 TDBA? = ? (MM)
11 PROMPT
12 1E3
13 /
14 STO Ø3
15 4
16 RCL Ø2
17 *
18 RCL Ø3
19 3
20 Y  X
21 *
22 TI = ?
23 PROMPT
24 STO Ø9
25 *
26 9,81
27 *
28 STO Ø4
29 1
30 ENTER
31 TTRANS = 1, OTHER = 2
32 PROMPT
33 X = Y?
34 GTO Ø3
35 1
36 ENTER
37 TTURB = 1, LAM = 2
38 PROMPT
39 X = Y?
40 GTO Ø5
41 RCL Ø3
42 X  2
43 9,81
44 *
45 RCL Ø9
46 *
47 RCL Ø1
48 /
49 1,05 E-6
50 /
51 GTO Ø4
52 LBL Ø5
53 RCL Ø3
54 9,81
55 *
56 RCL Ø9
57 *
58 RCL Ø2
59 /
60 SQRT
```

```
61 GTO Ø4
62 LBL Ø3
63 1,05 E-6
64 RCL Ø1
65 *
66 X  2
67 STO Ø5
68 RCL Ø4
69 +
70 SQRT
71 RCL Ø5
72 SQRT
73 -
74 2
75 /
7  RCL Ø2
77 /
78 RCL Ø3
79 /
80 LBL Ø4
81 TN = ?
82 PROMPT
83 STO Ø7
84 *
85 STO Ø6
86 TV =
87 XEQT BBB
88 RCL Ø6
89 RCL Ø3
90 *
91  RCL Ø7
92  /
93  1,05 E-6
94  /
95  TRE =
96  XEQT BBB
97  RCL Ø9
98  RCL Ø3
99  *
100 9,81
101 *
102 RCL Ø7
103 X  2
104 *
105 RCL Ø6
106 X  2
107 /
108 STO 10
109 TK =
110 XEQT BBB
111 1
112 ENTER
113 BEGIN = 1, NEW D = 2
114 PROMPT
115 X = Y?
116 GTO Ø1
117 GTO Ø2
18 END
```

E.8 Notes on the use of programs E.1 to E.6

(See special instructons in Section E.9 regarding program "PR")

As input a table of particle diameter d_j and their percentage of weight x_j of the total sample (or population) is required. If a grading curve is given, the mid value of an appropriately sized class interval can be taken. Try to use at least 4 to 5 class interval, (the more, the better the accuracy).

To run programs:

1 XEQ ^{T} PL (or SL, PT...)
  Display: D = ? or 999
2 Key in $_{\perp}$ (in millimetres)
3 R/S
  Display: $\wedge$ = ?
4 Key in x_1 (x_j 1,0)
5 R/S
  Display: D = ? or 999
6 Key in d_2 (in millimetres)
  ie repeat 2. to 5. until last x_j has been entered and pressed R/S
  Display: D = ? or 999
7 Key in 999
  Display: DPL = ab.cd (in millimetres)
  Answer.

E.9 Notes on the use of program E.5 "PR"

Here the effective particle diameter has to be solved for by iteration. The input data required are again d_j and x_j in addition to C_1, C_2 and the hydraulic gradient i. Note that these values are required for calculation purposes only and the results are not very sensitive to changes in the values.

To run program:

1 XEQ ^{T} PR
  Display: C2 = ? GEN = 4
2 Key in C_2
3 R/S
  Display I = ?
4 Key in hydraulic gradient i
5 R/S
  Display: C_1 = ? GEN = 800
6 Key in C
7 R/S
  Display: D = ? or 999
8 Go through slips 2. to 6. in the notes ont he use of programs H.1 to H.6
9 Key in 999
  Display: RHS = abc.d (value of RHS of equation)
10 R/S
  Display: TRIAL D = ?
11 Key in first guess at d_{PR}
12 R/S
  Display: %CH = $\pm$ ab.cd
  (This value indicates the percentage difference between the left and right hand sides of the equation)
13 R/S
  Display: OK = 1, NOT = 2
  14 If the percentage difference between the left and right hand sides is small enough, then key in 1 (for OK). If the percentage difference is too great, key in 2 (for NOT OK)

14(a) (ie 2 has been entered)

R/S

Display: TRIAL D = ?; ie back at step 10

Repeat until %CP minimised

14(b) (ie 1 has been entered after prompt OK = 1, NOT = 2)

R/S

Display DPR = ab.cd (in millimetres)

Answer

E.10 Notes on the use of program "VEL"

The effective particle diameters for laminar, transitional and turbulent flow are assumed to be known for either the parallel or series layer models (as deemed applicable)

1 XEQ VEL
  Display: C1 = ? CEN = 800
2 Key in C1
3 R/S
  Display: C2 = ? GEN = 4
4 Key in C_2
5 R/S
  Display DBAR = ? MM
6 Key in effective particle diameter (eg d_{PL})
7 R/S
  Display: I = ?
8 Key in hydraulic gradient i
9 R/S
  Display: TRANS = 1, OTHER = 2
10 Key in "1" if it is assumed that the flow falls within the TRANSitional regime, or key in "2" for either laminar or turbulent flow
11 R/S
  Display: (a) if choice "1" in step 10: N = ?
  (b) if choice "2" in step 10: TURB = 1, LAM = 2
12 Key in (a) porosity (N)
  (b) "1" if it is assumed the flow falls within the TURBulent regime; or "2" for laminar flow

13 R/S
  Of at (b) in step 12, then display is: N = ?
13 (a) Key in porosity (N)
  R/S
  Display now in both cases, after having keyed in the porosity (N): V = a.cde (velocity in m/S)

14 R/S

Display: RE = abcd.e (Reynolds number)

(Here the assumption on the flow regime can be checked:

RE < 64 : Laminar flow

64 < RE < 2000 - 4000 : Transitional flow

RE > 2000 - 4000 : Turbulent flow)

15 R/S

Display: K = a.bc (1 $\frac{idgn^2}{v^2}$ = friction factor)

if K C_2, then wrong type of equation, ie laminar instead of transitional or turbulent, was chosen

16 R/S

Display: BEGIN = 1, NEW D = 2

17 Key in "1" to go to step 1, ie to repeat all input

Key in "2" to go to step 5, ie to enter program again at input of new effective diameter - corresponding to choice of flow regime assumption.

Author Rumpelt T K
Name of thesis Performance of filter drains under large embankment loads 1983

PUBLISHER:
University of the Witwatersrand, Johannesburg
©2013

LEGAL NOTICES:

Copyright Notice: All materials on the University of the Witwatersrand, Johannesburg Library website are protected by South African copyright law and may not be distributed, transmitted, displayed, or otherwise published in any format, without the prior written permission of the copyright owner.

Disclaimer and Terms of Use: Provided that you maintain all copyright and other notices contained therein, you may download material (one machine readable copy and one print copy per page) for your personal and/or educational non-commercial use only.

The University of the Witwatersrand, Johannesburg, is not responsible for any errors or omissions and excludes any and all liability for any errors in or omissions from the information on the Library website.